CHAPTER 4

EXPERIMENTAL DURABILITY STUDY OF FRP COMPOSITE PILES

4.1 INTRODUCTION

The lack of long-term performance and durability data of composite piles is an important concern that must be addressed to permit confidence in use of these piles for long-term load-bearing applications. Consequently, a durability study was undertaken to assess the rate degradation of mechanical properties (strength and stiffness) of commercially available glass fiber reinforced polymer (GFRP) tubes used to fabricate concrete-filled FRP composite piles. The study focused on the degradation effects of moisture absorption and exposure to freeze-thaw cycles.

The durability study was carried out on four FRP tubes supplied by two manufacturers of FRP composite piles. The laboratory degradation study included FRP shell characterization, determination of baseline mechanical properties, measurement of moisture absorption as a function of time, measurement of mechanical properties as a function of moisture absorption, and mechanical properties as a function of exposure to freeze-thaw cycles. The methodology and results of this durability study are presented in this chapter. The durability study did not include the steel-reinforced plastic pile because this pile type was initially not included in the scope of this project, and was only included for field testing after the late withdrawal of one of the FRP composite pile manufacturers.

4.2 BACKGROUND ON DEGRADATION OF GLASS FRP COMPOSITES

Some of the factors that contribute to the degradation of the glass FRP (GFRP) composites over time include temperature, sunshine (UV rays), moisture absorption, freeze-thaw cycles, and load (Garcia et al. 1998, Nishizaki and Meiarashi 2002). Among

these factors, the influence of moisture absorption and exposure to freeze-thaw cycles are considered to be the most critical factors. Exposure to alkaline environments and ultra-violet (UV) radiation also affect long-term durability, but to a lesser extent. Furthermore, UV degradation resistance of most composites is being improved by applying protective coats and additives during the manufacturing process. The degradation mechanisms related to moisture absorption and freeze-thaw are discussed below.

Degradation due to moisture absorption may significantly reduce the life of FRP composites. The influence that moisture absorption has on the mechanical properties of GFRP composites is well documented (e.g. Shen and Springer 1976, Garcia et al. 1998, Prian and Barkatt 1999, Verghese et al. 1999, Shao and Kouadio 2002, Phifer 2003). Absorbed moisture can cause pronounced changes in modulus, strength, and strain to failure (Springer et al. 1980). Moisture content of submerged FRP composites increases through diffusion. The absorbed moisture can act as a plasticizer of the composite resin, and can cause matrix cracking, fiber-matrix debonding, and corrosion of glass fibers (stress corrosion) (Garcia et al. 1998). These effects result in a reduction of strength and stiffness of the FRP composite. For example, Phifer (2003) recorded tensile strength and stiffness reductions on the order of 60% and 10%, respectively, for E-glass/vinyl ester composites submerged in fresh water for a period of about 2 years. The author projected FRP tensile strength loss of about 80% after 50 years submergence. The implications of such strength reductions on the design of composite piles can be significant.

In addition to submergence time, temperature and stress level also influence the amount of moisture that FRP will absorb while submerged. The moisture absorption increases with increasing water temperature and stress level. Evidence of the existence of damage to FRP composites after submergence in water has been found in scanning electron microscope (SEM) images (e.g., Figure 2.9), where fiber damage and crack formation at the fiber-matrix interface was observed (McBagonluri et al. 2000).

Freeze-thaw cycles can also degrade FRP composite properties. The degradation due to freeze-thaw cycling is primarily related to microcracking caused by the volume increase

of the absorbed water in the composite (Verghese et al. 1999). The mechanical properties of the composite are also affected by cold temperatures and by the cycling process (Karbhari 2002).

The FRP shell will potentially be exposed to chemical agents as a result of the alkaline pore water from the concrete inside the FRP shell. Karbahari et al. (2002) studied the effect of concrete based alkali solutions on the durability of vinylester GFRP composites. The authors found evidence of significant degradation and strength loss due not only to moisture absorption, but also due to the exposure to the high pH levels and characteristic solution chemistry of concrete pore fluid. The experimental durability program carried out for this study did not include investigation of possible degradation effects due to exposure to concrete pore fluid solutions.

A concrete-filled FRP composite pile installed in tidal and marine environments would be exposed to salt water. However, McBagonluri et al. (2000) found that the rate of strength loss was not significantly affected by salt content but rather by absorption of moisture. Therefore, the durability experiments carried out for this study were performed using fresh water.

4.3 LABORATORY STUDY OF DURABILITY

The general approach used in this study was to track moisture diffusion into the material and to evaluate the degradation of the mechanical properties of the different FRP shells as a function of submergence time and moisture absorption. The material strength and stiffness loss is then related to the long term structural capacity of the pile using conventional structural models for FRP composite piles available in the literature (e.g. Fam and Rizkalla 2000, Mirmiran 1999) and summarized in Chapter 2. The study described herein does not include effects of creep or chemical attack as a result of the presence of the concrete infill in the composite pile. Changes of the concrete properties with time, i.e., possible increases or decreases in strength and/or stiffness, were not included in this study.

4.3.1 Description of test specimens

Commercially-available FRP tubes from two manufacturers that specialize in concrete-filled FRP composite piles (Lancaster Composites and Hardcore Composites, Inc) were used for the durability experimental program. Tubes with 0.305 m (12 in) and 0.610 m (24 in) nominal diameter were tested. The test results presented herein are based on tests carried out on their standard FRP tube designs. It should be noted, however, that both pile manufacturers have the flexibility to modify the FRP composite shell laminate architecture (including number of layers, fiber orientation, and resin and fiber types) to better suit the load demands of a specific project.

The following subsections provide detailed descriptions of the tubes from each manufacturer, including dimensions, material, number of layers, laminate structure, fiber volume fraction, and manufacturing technique.

4.3.1.1 Specimens from Lancaster Composites Inc.

The two sizes of tubes supplied by Lancaster composites, Inc. were fabricated by the Fiberglass Composite Pipe Division of the Ameron International Corporation. The FRP tubes were manufactured using the filament-winding technique, where E-Glass continuous fiber rovings are impregnated with resin (epoxy or polyester) and wound over a rotating steel mandrel, following a predetermined winding pattern.

Characterization of the FRP tubes was based on visual inspection, information supplied from the manufacturers, and burnoff tests on coupon samples. The burnoff tests were performed in general accordance with ASTM Standard D2584. The burnoff test results and other characterization information are provided in Tables 4.1 and 4.2 for the 12- and 24-inch diameter tubes, respectively.

Table 4.1 Characterization data for Lancaster Composites Inc. 12-inch FRP Tube

Manufacturer pile designation	CP40 12-inch
Nominal diameter	305 mm (12 in)
Measured outside diameter	324.7 ± 1.9 mm (1)
Total wall thickness	6.05 ± 0.14 mm (1)
Liner thickness	0.59 ± 0.05 mm (1)
Liner material	Epoxy resin sandwiched between industrial paper
Unit weight of tube	17.45 kN/m^3
Fiber type	Owen Corning Type 30 113 Yield E-glass
Matrix resin type	Epoxy anhydrite hardener/Dow Der 331 (83/100 ratio)
Fiber layup angles	$[-88^o/+8^o/-88^o/+8^o/-88/+8^o/-88^o/+8^o/-88]_T$ (2)
Fiber layer average thicknesses	[0.54/0.69/0.54/0.69/0.54/0.69/0.54/0.69/0.54] (mm)
Total resin fraction by weight	38.6 %
Total fiber fraction by volume	45.8 ± 1.0 % (1), (3)
Fiber volume fraction 88^o layers	38.4 ± 1.0 % (1)
Fiber volume fraction 8^o layers	55.8 ± 0.3 % (1)
Percentage of fiber at 88^o	40.1 ± 0.6 % (1) (by weight)
Percentage of fiber at 8^o	59.9 ± 0.6 % (1) (by weight)

Notes: (1): Mean ± standard deviation.
(2): Angles are measured with respect to pile longitudinal axis. Subscript "T" indicates orientation for the layers of the total laminate are presented within the brackets.
(3): Based on volume of FRP laminate only, i.e., liner is excluded from volume.

Table 4.2 Characterization data for Lancaster Composites Inc. 24-inch FRP Tube

Manufacturer pile designation	CP40 24-inch
Nominal diameter	610 mm (24 in)
Measured outside diameter	625 ± 1.8 mm (1)
Total wall thickness	7.35 ± 0.23 mm (1)
Liner thickness	1.68 ± 0.09 mm (1)
Liner material	C-veil, a chopped fiber mat and resin
Unit weight of tube	17.36 kN/m^3
Fiber type	Owen Corning Type 30 113 Yield E-glass
Matrix resin type	Ashland Chemical Apropol 7241 isophtalic acid polyester resin
Fiber layup angles	$[+35^o/-35^o/+85^o/+35^o/-35^o]_T$ (2)
Fiber layer average thicknesses	[1.13/1.13/1.13/1.13/1.13] (mm)
Total resin fraction by weight	39.3 %
Total fiber fraction by volume	51.2 ± 2.4 % (1), (3)
Fiber volume fraction ± 35^o layers	52.7 ± 2.9 % (1)
Fiber volume fraction 85^o layer	45.5 ± 1.0 % (1)

Notes: (1): Mean ± standard deviation.
(2): Angles are measured with respect to pile longitudinal axis. Subscript "T" indicates orientation for the layers of the total laminate are presented within the brackets.
(3): Based on volume of FRP laminate only, i.e., liner is excluded from volume.

The 0.305 m (12-inch) nominal diameter tube has an outer diameter of 325 mm (12.8 in.) and an average total wall thickness of 6.05 mm (0.238 in.). The tube has a 0.59 mm (0.023 in.) thick liner at the inner surface, which results in a net structural wall thickness of 5.46 mm (0.215 in.). The wall structure of the tube consists of nine layers of fibers oriented at – 88 degrees and + 8 degrees with respect to the longitudinal axis of the tube. The stacking sequence of the layers is $[-88^{o}/+8^{o}/-88^{o}/+8^{o}/-88/+8^{o}/-88^{o}/+8^{o}/-88^{o}]_{T}$ (subscript T indicates the stacking sequence for the total FRP laminate is presented within the brackets). The layers with fibers oriented at -88 degrees with respect to the longitudinal axis are 0.54 mm (0.021 in.) thick, and the layers with fibers oriented at +8 degrees with are 0.69 mm (0.027 in.). The FRP tube liner is composed of overlapped industrial paper impregnated with epoxy resin and is about 0.59 mm (0.023 in.) thick. The average overall fiber volume fraction of this tube is 45.8 %. The matrix resin for this FRP tube consisted of DOW Der 331 epoxy mixed with anhydrite hardener. The fiber type was Owens Corning Type 30 113 Yield E-Glass rovings.

The 0.610 m (24-inch) nominal diameter tube has an outer diameter of 625 mm (24.6 in.) and an average total wall thickness of 7.35 mm (0.289 in.). The tube has a 1.68 mm (0.066 in.) thick liner at the inner surface, which results in a net structural wall thickness of 5.67 mm (0.223 in.). The wall structure of the tube consists of five layers of fibers oriented at $[+35^{o}/-35^{o}/+85^{o}/+35^{o}/-35^{o}]_{T}$, measured with respect to the longitudinal axis of the tube. The fiber layers are about 1.13 mm (0.044 in.) thick. The FRP tube liner is composed of C-veil and a mat of chopped fiber impregnated with resin, and is about 1.68 mm (0.066 in.) thick. The average overall fiber volume fraction of this tube is 51.2 %. The matrix resin for the 0.610 m (24 in.) FRP shell was isophthalic acid polyester resin (Ashland Chemical Apropol 7241). The fiber type was Owens Corning Type 30 113 Yield E-Glass rovings.

4.3.1.2 Specimens from Hardcore Composites Inc.

Two FRP tube sizes were supplied by Hardcore Composites LLC, Inc. The tubes had 12-inch and 24-inch nominal diameters and were fabricated at their manufacturing plant in

New Castle, Delaware. Both FRP tubes sizes were fabricated using a Vacuum Assisted Resin Transfer Molding (VARTM) process. The matrix resin used in the tubes is Dow vinyl ester Derakane resin, and the fiber reinforcing consists of plies of stitch-bonded multi-axis glass fiber fabric. Each ply includes four layers of fibers oriented at 0, +45, -45, and 90 degrees with respect to the longitudinal axis of the tube.

Characterization of the FRP tubes was based on visual inspection, information supplied from the manufacturer, and burnoff tests performed on coupon samples. The burnoff tests were carried out in general accordance with ASTM Standard D2584. Characterization information, including burnoff test results, are provided in Tables 4.3 and 4.4 for the 12- and 24-inch diameter tubes, respectively.

Table 4.3 Characterization data for Hardcore Composites, Inc. 12-inch FRP Tube

Manufacturer pile designation	12-3
Nominal diameter	305 mm (12 in)
Measured outside diameter	321.7 ± 3.8 mm (1)
Total wall thickness	5.66 ± 0.28 mm (1)
Liner thickness	0.68 ± 0.11 mm (1)
Liner material	Screen
Unit weight of tube	18.6 kN/m^3
Fiber type	E-glass multi-axis fabric type Quad Q-9100. 4 stitched layers oriented at [0°/+45°/-45°/90°] (2)
Matrix resin type	Dow vinyl ester Derakane resin
Number of multiaxis plies	3 x [0°/+45°/-45°/90°] (2)
Multi-axis fiber layer thicknesses	1.66 ± 0.11 mm (1)
Total resin fraction by weight	28.2 %
Total fiber fraction by volume	52.8 ± 0.1 % (1), (3)
Fiber volume fraction 0° layers	60.6 ± 2.6 % (1)
Fiber volume fraction ±45° layers	41.7 ± 6.7 % (1)
Fiber volume fraction 90° layers	34.2 ± 8.3 % (1)
Percentage of fiber at 0°	56.1 ± 1.4 % (1) (by weight)
Percentage of fiber at ±45°	37.1 ± 1.1 % (1) (by weight)
Percentage of fiber at 90°	6.8 ± 0.3 % (1) (by weight)

Notes: (1): Mean ± standard deviation. (2): Angles are measured with respect to pile longitudinal axis.
(3): Based on volume of FRP laminate only, i.e., liner is excluded from volume.

Table 4.4 Characterization data for Hardcore Composites, Inc. 24-inch FRP Tube

Manufacturer pile designation	24-4
Nominal diameter	610 mm (24 in) outside
Measured outside diameter	622 ± 1.6 mm (1)
Total wall thickness	8.86 ± 0.68 mm (1)
Liner thickness	0.68 ± 0.15 mm (1)
Liner material	Screen
Unit weight of tube	18.67 kN/m^3
Fiber type	E-glass multi-axis fabric type Quad Q-9100. 4 stitched layers oriented at [0°/+45°/-45°/90°] (2)
Matrix resin type	Dow vinyl ester Derakane resin
Number of multi-axis plies	4 x [0°/+45°/-45°/90°] (2)
Multi-axis fiber layer thicknesses	2.05 ± 0.14 mm (1) (mm)
Total resin fraction by weight	28.6 %
Total fiber fraction by volume	52.1 ± 0.5 % (1), (3)
Fiber volume fraction 0° layers	61.2 ± 1.4 % (1)
Fiber volume fraction ±45° layers	45.2 ± 0.6 % (1)
Fiber volume fraction 90° layers	40.7 ± 1.1 % (1)
Percentage of fiber at 0°	53.9 ± 0.7 % (1) (by weight)
Percentage of fiber at ±45°	38.9 ± 0.8 % (1) (by weight)
Percentage of fiber at 90°	7.3 ± 0.1 % (1) (by weight)

Notes: (1): Mean ± standard deviation. (2): Angles are measured with respect to pile longitudinal axis.
(3): Based on volume of FRP laminate only, i.e., liner is excluded from volume.

The 305 mm (12-inch) nominal diameter tube has an outer diameter of 322 mm (12.7 in.) and a total wall thickness of 5.66 mm (0.223 in.). The tube has a 0.68 mm (0.027 in.) thick liner at the inner surface, which results in a net structural wall thickness of 4.98 mm (0.196 in.). The wall structure of the tube consists of 3 layers of multi-axis fabric. Each fabric layer consists of 4 layers of fibers oriented at [0°/90° /+45 °/-45°]. The symbol typically used to designate this fiber lay-up is $[0^o/90^o/+45^o/-45^o]_{3T}$ (where the subscript "3T" indicates the FRP laminate is composed of three plies each with four layers oriented at 0°/90° /+45 °/-45°). The average thickness of the multi-axis fabric layers is 1.66 mm (0.065 in.). The average thicknesses of the layers with fibers oriented at ± 45, 0, and 90 degrees, with respect to the longitudinal axis of the tube, are 0.74 mm (0.029 in.), 0.76 mm (0.030 in.), and 0.16 mm (0.006 in.), respectively. The FRP tube liner is composed of a plastic screen material used to facilitate the injection of resin during the manufacturing process. The average overall fiber volume fraction of these tubes was measured to be 52.8 %.

The 610 mm (24-inch) nominal diameter tube has an outer diameter of 622 mm (24.5 in.) and a total wall thickness of 8.86 mm (0.349 in.). The tube has a 0.68 mm (0.027 in.) thick liner at the inner surface, which results in a net structural wall thickness of 8.18 mm (0.322 in.). The wall structure of the tube consists of 4 layers of multi-axis fabric. Each fabric layer consists of 4 layers of fibers oriented at [0^o/90^o /+45 ^{o}/-45^o]. The symbol typically used to designate this type of fiber lay-up is [0^o/90^o /+45 ^{o}/-45^o]$_{4T}$ (where the subscript "4T" indicates the FRP laminate is composed of four plies each with four layers oriented at 0^o/90^o /+45 ^{o}/-45^o). The average thickness of the multi-axis fabric layers is 2.05 mm (0.081 in.). The average thicknesses of the layers with fibers oriented at ± 45, 0, and 90 degrees, with respect to the longitudinal axis of the tube, are 0.92 mm (0.036 in.), 0.94 mm (0.037 in.), and 0.19 mm (0.007 in.), respectively. The average overall fiber volume fraction of these tubes was measured to be 52.1 %.

4.3.2 Test Equipment and Procedures

The test procedures and apparatus used in this durability study are described below.

4.3.2.1 Burnoff tests

As indicated earlier, coupons from the different FRP tubes investigated were subjected to burnoff tests to determine information such as fiber volume content, resin content, the number of fiber layers and orientations. The tests were carried out in general accordance with ASTM Standard D2584. The tests consist of heating coupon samples from the FRP tubes in a furnace oven to a temperature of about 550 ^{o}C. The heat from the oven is used to burn the resin matrix leaving the fiber layers exposed. The oven used for burnoff testing is shown in Figure 4.1a. A FRP coupon sample after resin burnoff is shown in Figure 4.1b. The number of fiber layers and orientation can be obtained from this test as shown in Figure 4.1b.

a) Oven used for burnoff testing

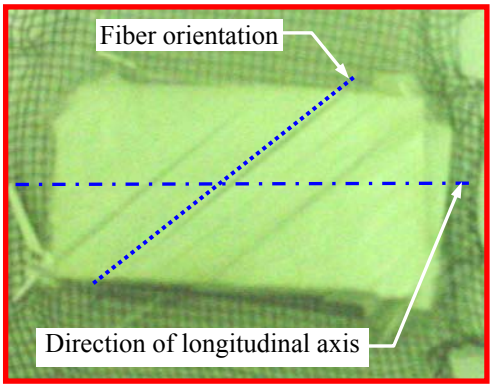

b) Sample after resin burnoff

Figure 4.1 Burnoff testing

4.3.2.2 Axial tension tests

Axial tensile properties were evaluated using tensile tests performed on FRP samples in accordance with ASTM Test Method for Tensile Properties of Polymer Matrix Composite Materials (D3039). Test specimen strips were cut in the longitudinal direction using a water-cooled saw. The average test specimen dimension was 25 mm x 200 mm. The tests were carried out using an Instron test frame operated at a constant rate of displacement of 1.27 mm/min (0.05 in/min). Axial strain was measured primarily with the use of extensometers, however selected samples were also instrumented with strain gages. A typical tension test setup is shown in Figure 4.2.

Figure 4.2 Typical tension test setup

4.3.2.3 Hoop tension tests

Tensile properties in the hoop direction were evaluated using the split disk test method. The split disk fixtures were custom made to fit the two FRP tube diameter sizes investigated in this study. The split disk tests were performed in accordance with ASTM Test Method for Apparent Hoop Tensile Strength of Plastic or Reinforced Plastic Pipe by Split Disk Method (D2290). Split disk specimens were precision cut from the FRP shells at the Strongwell Corporation in Bristol, VA. The FRP ring specimens had a nominal width of 40 mm. The tests were carried out using a 534 kN Tinius-Olsen machine and an Instron test frame at a constant rate of displacement of 2.5 mm/min (0.1 in/min). The typical split disk test setup is shown in Figure 4.3.

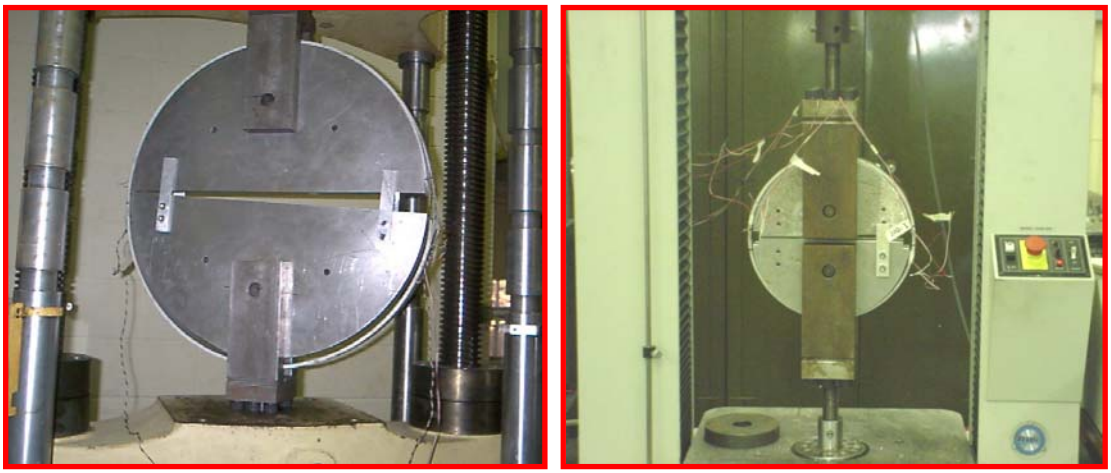

a) 24-inch split disk fixture b) 12-inch split disk fixture

Figure 4.3 Typical split disk test setup

4.3.2.4 Freeze-Thaw Testing

Saturated FRP specimens were subjected to freeze-thaw cycles using the programmable Blue-M Freeze-Thaw Chamber shown in Figure 4.4.

Figure 4.4 Freeze-thaw chamber

The FRP specimens were fitted into special freeze-thaw fixtures which loaded the specimens in 4-point bending. This arrangement was chosen to approximate the bending moment present in piles near the pile cap. The fixture used is shown in Figure 4.5. Use of this fixture resulted in tensile strains in the outer extreme fiber of the 24-inch diameter tube specimens ranging from 2800 to 5500 microstrains. The specimens from the 12-inch tubes were subjected to freeze-thaw cycles in an unloaded state, i.e., unstrained. The chamber was programmed to produce approximately 10 freeze-thaw cycles per day. A typical freeze-thaw cycle is shown in Figure 4.6. Specimens were subjected to 100, 300, and 500 freeze-thaw cycles. As a point of interest, SW Virginia experiences about 50 freeze-thaw cycles per year, i.e., 500 freeze-thaw cycles in about 10 years.

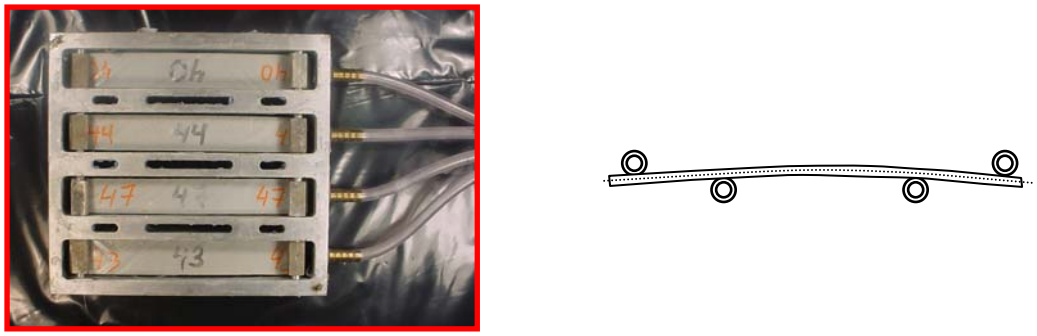

a) Lancaster 24-inch specimens **b) Loaded sample in 4-point bending**

Figure 4.5 Freeze-thaw fixture

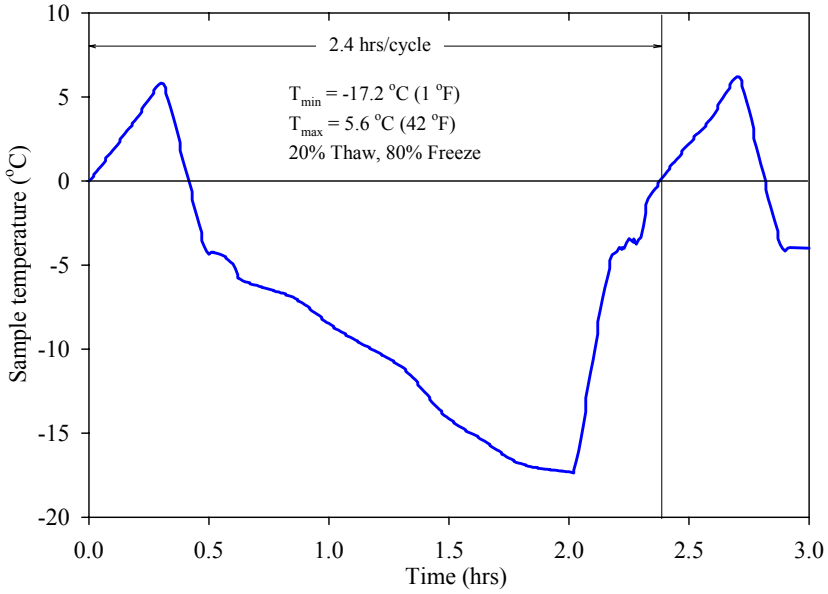

Figure 4.6 Average freeze-thaw cycle undergone by FRP samples

More details on the freeze-thaw study are given in the results section presented later in this chapter.

4.3.3 Baseline mechanical properties

In order to study the durability and long-term performance of FRP composite piles, it was necessary to first evaluate the baseline mechanical properties of the FRP shell in the longitudinal (axial) and hoop directions.

4.3.3.1 Longitudinal tension

The baseline properties of each pile type were obtained from a series of longitudinal tension tests, and the results are summarized in Table 4.5. Typical stress-strain curves obtained from these tests for each FRP type are shown in Figure 4.7.

Table 4.5 As-received longitudinal tensile properties

Property		Lancaster FRP		Hardcore FRP tube	
		24-inch	12-inch	24-inch	12-inch
Tensile strength (MPa) (1)	Mean	113.1	249.3	432.2	494.3
	SD (3)	7.3	17.7	46.9	60.6
Peak strain (%)	Mean	1.02	1.70	1.86	1.78
	SD	0.1	0.25	0.27	0.12
Initial modulus (GPa) (2)	Mean	14.8	23.2	27.3	29.6
	SD	1.9	2.1	3.15	0.9
Number of specimens	N	29	9	9	5

Notes: (1): Strength calculated using total thickness of FRP tube (includes liner).
(2): Initial modulus calculated between 0 and 4000 microstrain.
(3): SD = Standard deviation.

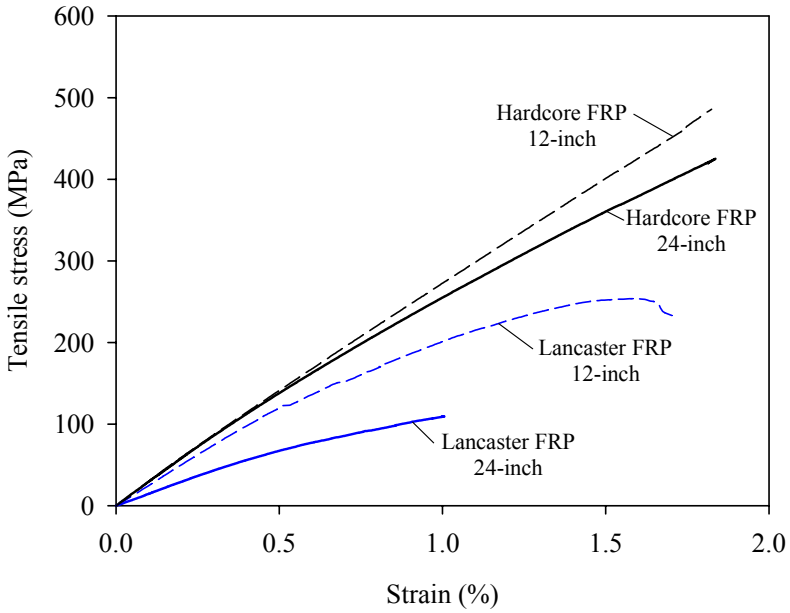

Figure 4.7 Representative baseline longitudinal tension stress-strain curves

4.3.3.2 Hoop tension

The baseline hoop tensile properties for the composite piles are summarized in Table 4.6. Typical stress-strain curves obtained from split disks tests are shown in Figure 4.8.

Table 4.6 As-received hoop tensile properties

Property		Lancaster FRP		Hardcore FRP
		24-inch	12-inch	12-inch
Tensile strength (MPa) (1)	Mean	121.4	195.2 (2)	93.5
	SD (5)	5.9	15.9	7.9
Peak strain (%)	Mean	1.26 (3)	1.28	1.45
	SD	0.34	0.10	0.40
Initial modulus (GPa) (4)	Mean	19.1	16.5	11.9
	SD	2.3	2.2	3.1
Number of specimens	N	5	11	5

Notes: (1): Strength calculated using total thickness of FRP tube (includes liner).
(2): The strain and modulus values are based only on the second batch of tests that used inner and outer strain gages (5 tests).
(3): No inner gages were used for this test batch; hence strain values are from outer gages only.
(4): Initial modulus calculated between 0 and 4000 microstrain.
(5): SD = Standard deviation.

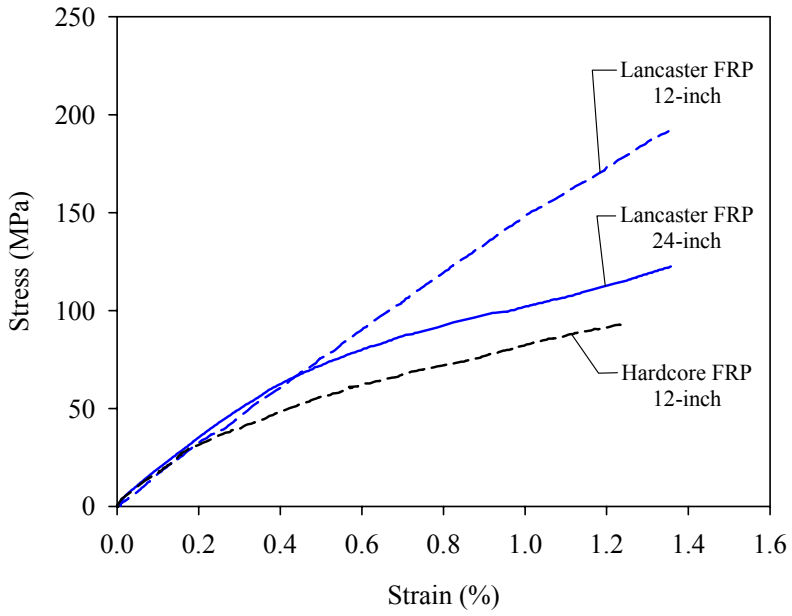

Figure 4.8 Representative baseline hoop tension stress-strain curves

It was not possible to perform split disk tests on the 24-inch Hardcore FRP shell specimens due to the non-circular shape of the inside of these shell. Hardcore shells have several resin transfer tubes attached to the inner wall (running longitudinally) that are used to inject the resin into the composite during manufacturing of the FRP shell, and at the end of the process, the tubes are left in place filled with resin. The size and number of these tubes made it impractical to test these specimens as the internal clearance is not circular.

4.3.4 Properties as a function of submergence time and moisture

4.3.4.1 Moisture absorption tests

Moisture absorption iso-thermal curves were obtained by immersing samples in fresh water tanks at the following temperatures: 22° C, 35° C, 45° C, 55° C, 65° C, and 80° C. The submerged FRP coupons were about 100 mm long and 25 mm wide, with their edges epoxy-coated to promote 1-D diffusion. Plots of moisture absorption versus time, for the 12-inch and 24-inch diameter Lancaster FRP shells, are shown in Figures 4.9 and 4.10,

respectively. Moisture absorption plots, for the 12-inch and 24-inch diameter Hardcore FRP shells, are shown in Figures 4.11 and 4.12, respectively. The moisture content, shown in these figures, corresponds to the percent weight gain with respect to the initial weight of the samples before submergence.

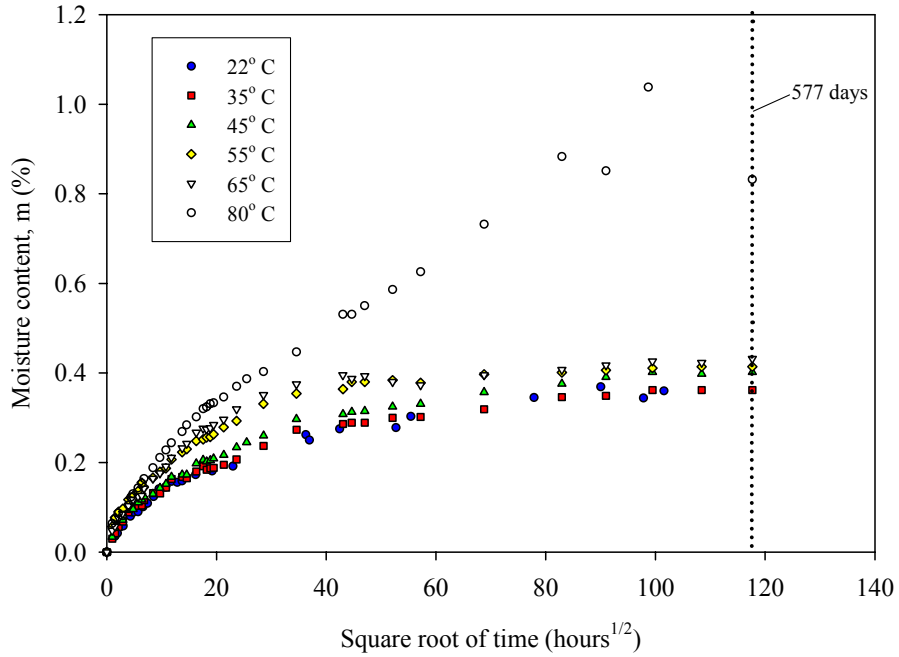

Figure 4.9 Absorption curves for Lancaster 12-inch FRP tube

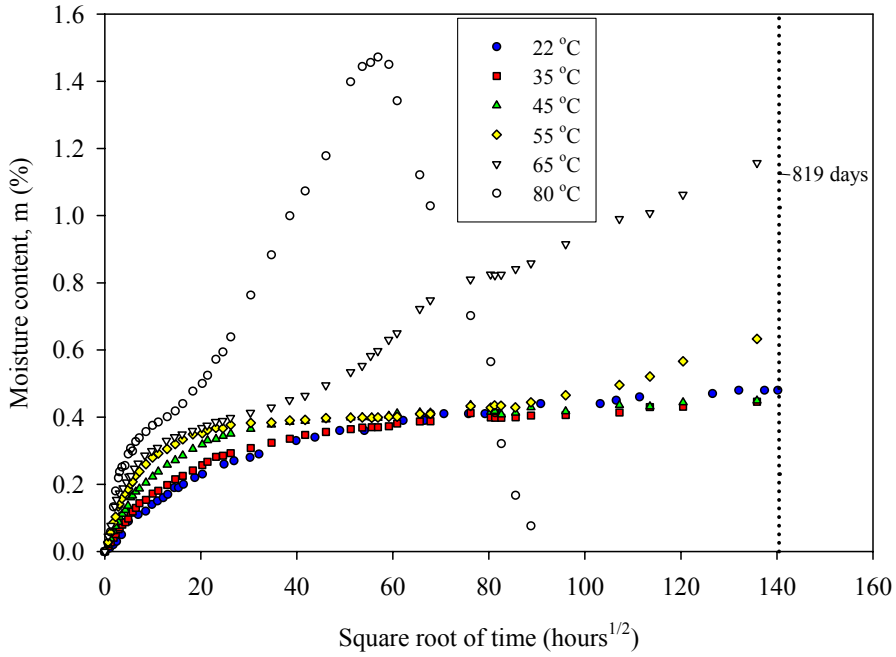

Figure 4.10 Absorption curves for Lancaster 24-inch FRP tube

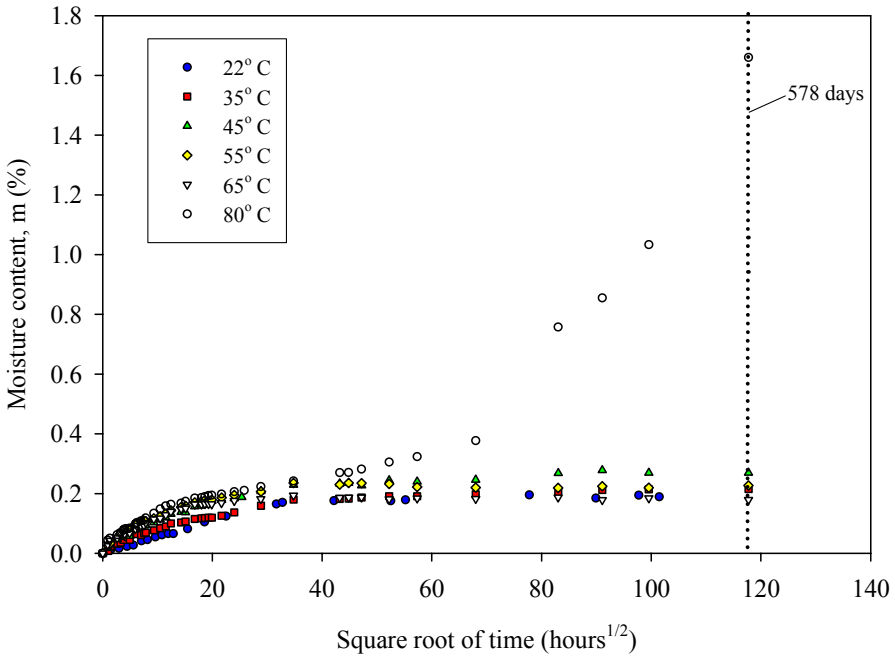

Figure 4.11 Absorption curves for Hardcore 12-inch FRP tube

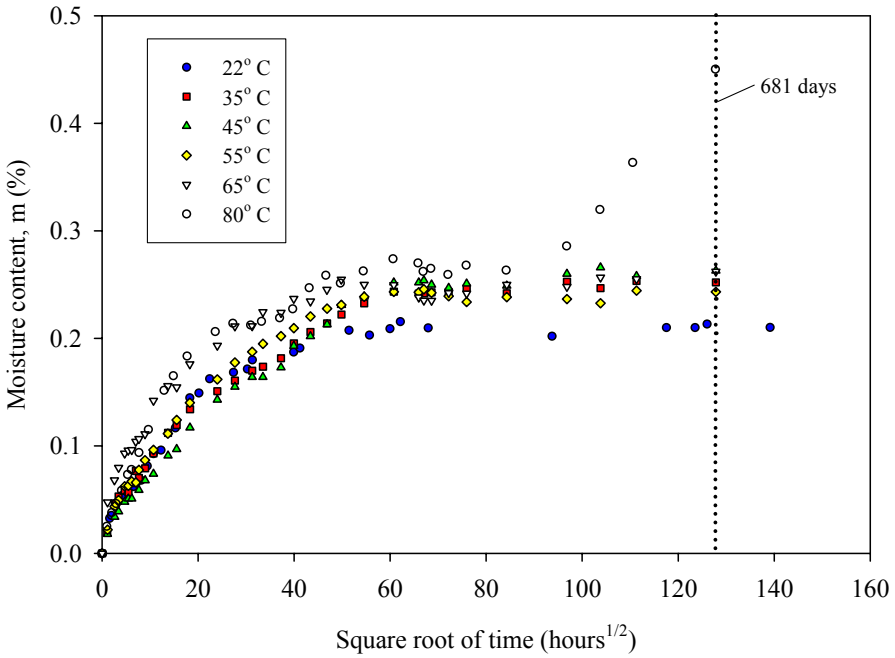

Figure 4.12 Absorption curves for Hardcore 24-inch FRP tube

All moisture absorption tests showed a rapid gain of weight at the start of the experiments, with the rate of increase being the greatest for the highest temperature of

80° C. With time, most of the tests below 65° C stabilized, reaching a saturation or equilibrium moisture content. For the tests at 80° C, the weights either continued to increase gradually, or in some cases, like the Lancaster 24-inch at 80° C, they started to decrease sharply in weight after reaching a peak. Nishizaki and Meiarashi (2002) reported similar decreases in moisture content for samples submerged at high temperatures. The authors attributed this behavior to loss of material from the composite matrix. The Lancaster 24-inch samples with water temperatures between 55 and 65° C seem to have a non-Fickian or two stage absorption behavior. Phifer (2003) found that, in some cases, Langmuirian diffusion predicts the behavior of E-glass vinyl ester composites better than Fickian diffusion. Diffusion analyses using Fickian and Langmuirian models are presented in the following subsection.

4.3.4.2 Diffusion properties

Two types of diffusion models were used to fit the experimental absorption data: Fickian and Langmuirian. These models are described briefly below.

The Fickian diffusion model is commonly used to predict moisture absorption of composite materials. This model has the convenience of being simple. The model assumes a constant diffusivity, D, and a saturation moisture, M_∞, to which the sample tends to as the submergence time increases. The expression for Fickian diffusion of a thin plate of thickness, h, is given by the following expression (Shen and Springer 1976):

$$M(t) = M_\infty \cdot \left[1 - \sum_{n=0}^{\infty} \frac{8}{(2n+1)^2 \pi^2} \cdot e^{-D(2n+1)^2 \pi^2 t / h^2} \right] \tag{4.1}$$

where $M(t)$ = moisture content of the FRP specimen at submergence time, t,

M_∞ = moisture content at saturation,

t = time of submergence,

D = diffusivity through the thickness of the FRP specimen,

h = thickness of FRP specimen.

Gurtin and Yatomi (1979) proposed using a Langmuirian diffusion model for FRP composites exhibiting non-Fickian absorption behavior. The following expression is given to track the moisture content of specimens following Langmuirian diffusion:

$$M(t) = M_{\infty} \cdot \left[1 - \left(\frac{\beta}{\alpha + \beta} \right) \cdot e^{-\alpha t} - \frac{\alpha}{\alpha + \beta} \cdot \sum_{n=0}^{\infty} \frac{8}{(2n+1)^2 \pi^2} \cdot e^{-D(2n+1)^2 \pi^2 t / h^2} \right] \qquad (4.2)$$

where M(t) = moisture content of the FRP specimen at submergence time, t,

M_{∞} = the Fickian moisture content at saturation,

t = time of submergence,

D = the Fickian diffusivity through the thickness of the FRP specimen,

α and β = constants usually obtained from curve fitting,

h = thickness of the FRP specimen.

The similarity of this model to the Fickian is evident from comparing Equations 4.1 and 4.2. The first none unity term in Equation 4.2 is indicative of a two-stage diffusion process. More details on the Langmuirian model can be found in Gurtin and Yatomi (1979).

Curve fits using the Fickian and Langmuirian models were perfomed on the experimental moisture absorption data gathered for the different FRP shells evaluated in this study. The curve fits for water temperatures 22^{o} C, 45^{o} C, and 65^{o} C are shown in Figures 4.13 and 4.14, for the 12-inch and 24-inch diameter Lancaster FRP shells, respectively. Fits for these same water temperatures, for the 12-inch and 24-inch diameter Hardcore FRP shells, are shown in Figures 4.15 and 4.16, respectively.

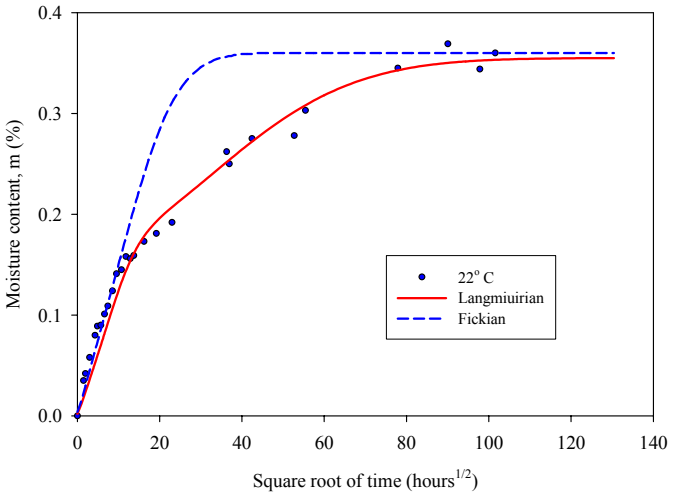

a) Water at 22° C

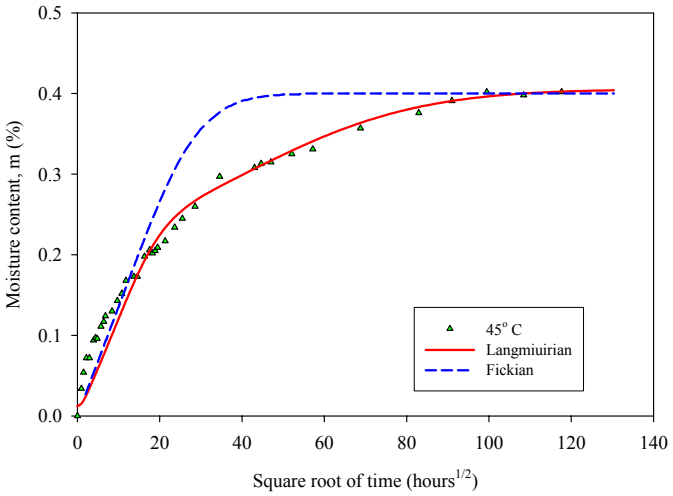

b) Water at 45° C

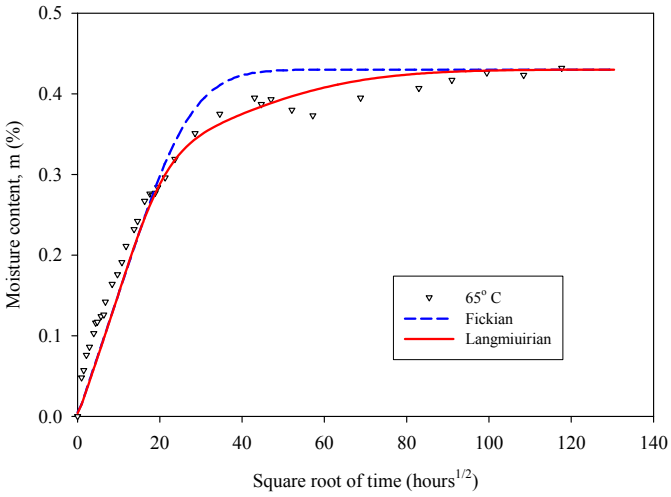

c) Water at 65° C

Figure 4.13 Selected diffusion analyses for Lancaster 12-inch FRP samples

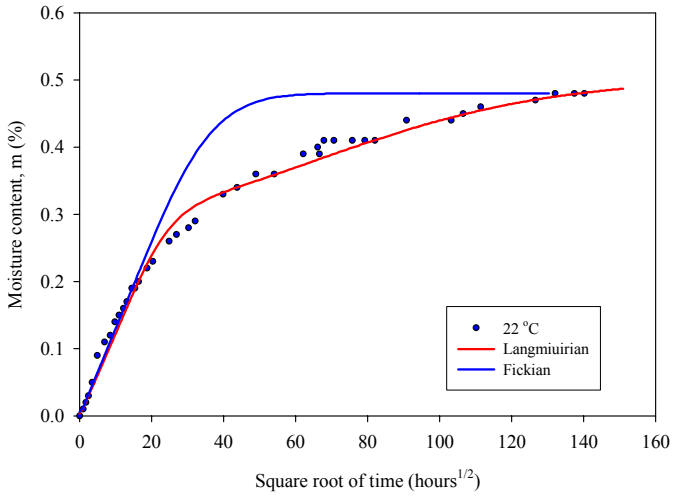

a) Water at 22° C

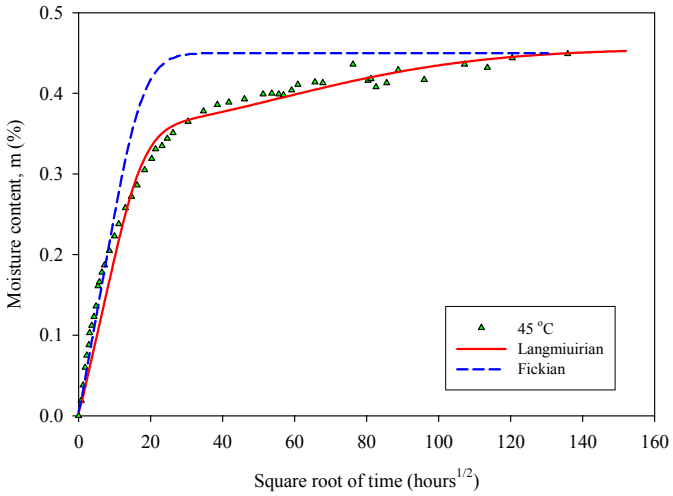

b) Water at 45° C

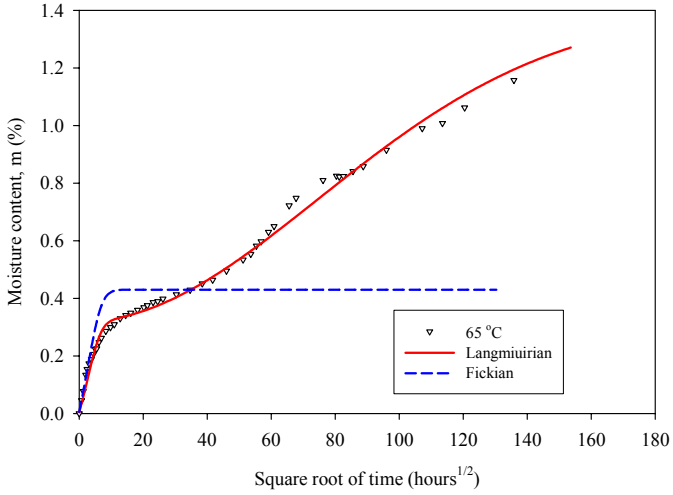

c) Water at 65° C

Figure 4.14 Selected diffusion analyses for Lancaster 24-inch FRP samples

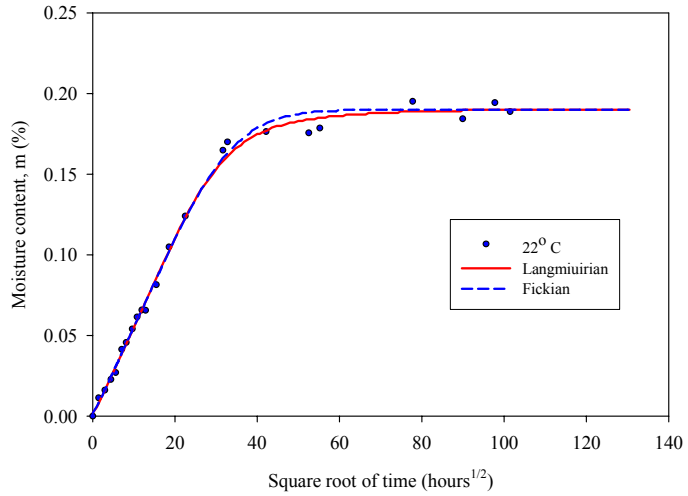

a) Water at 22^{o} C

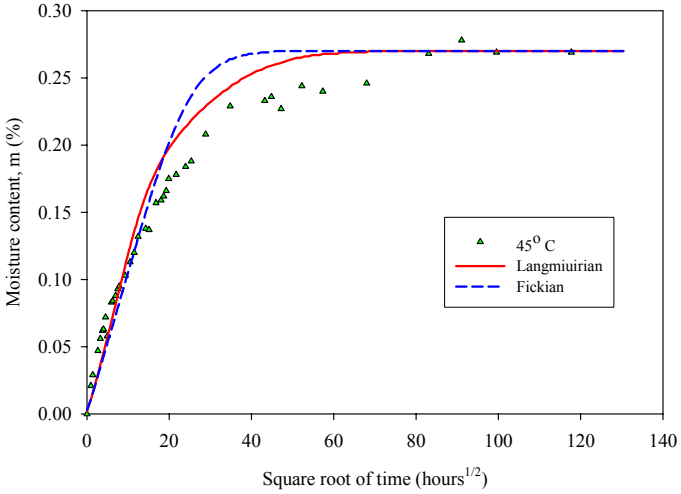

b) Water at 45^{o} C

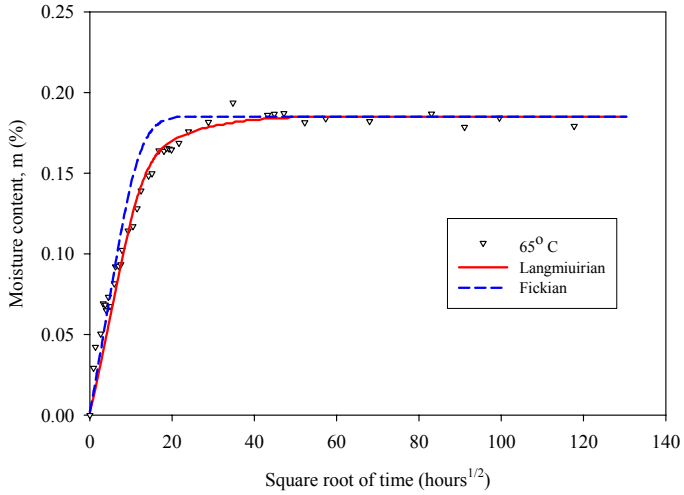

c) Water at 65^{o} C

Figure 4.15 Selected diffusion analyses for Hardcore 12-inch FRP samples

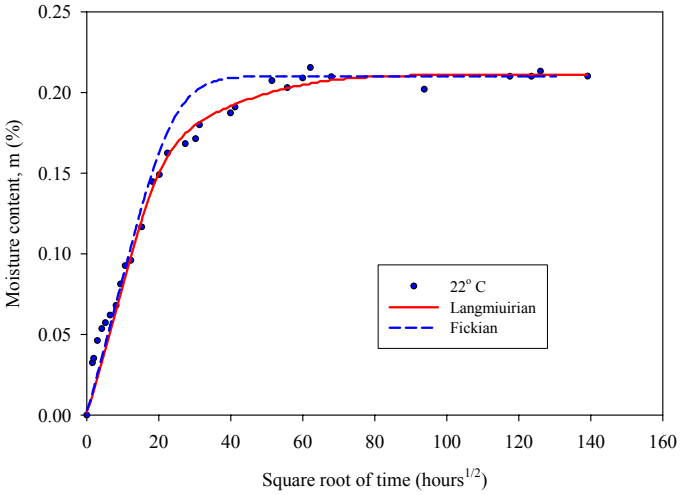

a) Water at 22° C

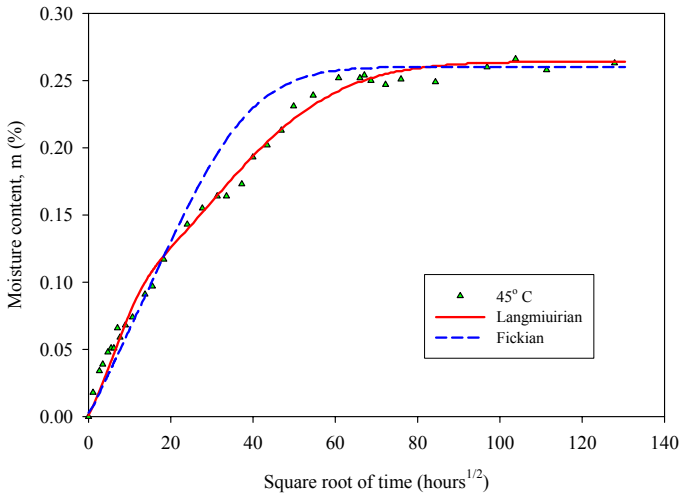

b) Water at 45° C

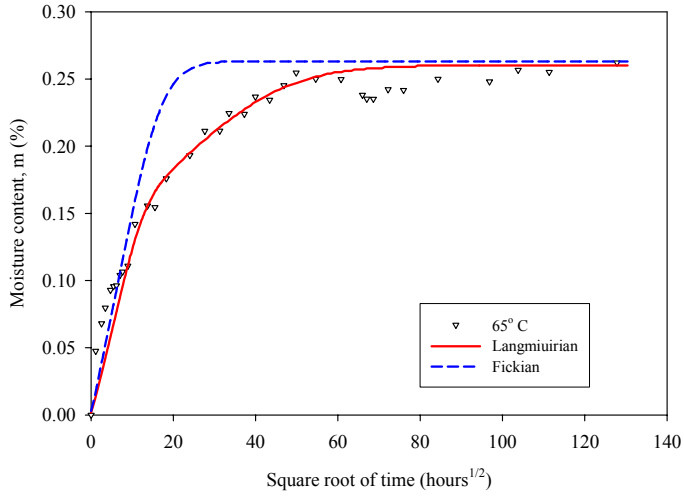

c) Water at 65° C

Figure 4.16 Selected diffusion analyses for Hardcore 24-inch FRP samples

These figures indicate that Langmuirian diffusion, which has four curve-fitting parameters (D, M_∞, α, β), is better able to track the measured moisture absorption than the Fickian diffusion, which has two-curve fitting parameters (D, M_∞), for samples submerged at temperatures between 55 and 80^o C.

The diffusivity (or diffusion coefficient D), and the saturation moisture content (M_∞) obtained from Fickian diffusion analyses are summarized in Tables 4.7 through 4.10, for the Lancaster 12-inch, Lancaster 24-inch, Hardcore 12-inch, and Hardcore 24-inch, respectively. Although there is much scatter in the values, it can be seen in the tables that the diffusivity and the saturation moisture tend to increase with temperature. Even though Langmuirian diffusion provided a better fit to the data, the Fickian model and parameter values are used for predicting the long term composite pile strength, as described later in this chapter, because of the simplicity of the Fickian model.

Table 4.7 Fickian diffusion parameters for the Lancaster 12-inch FRP

Water temperature (^{o} C)	Diffusivity, D (cm^2/hr)	Saturation moisture, M_∞ (%)
22	1.25 E-4	0.36
35	1.53 E-4	0.36
45	8.57 E-5	0.40
55	1.21 E-4	0.42
65	9.22 E-5	0.43
80	3.38 E-5	0.87 (1)

Notes: (1): Did not stabilize at the end of test, value is only used for curve fitting Fickian curves to data.

Table 4.8 Fickian diffusion parameters for the Lancaster 24-inch FRP

Water temperature (^{o} C)	Diffusivity, D (cm^2/hr)	Saturation moisture, M_∞ (%)
22	1.23 E-5	0.48
35	2.04 E-5	0.45
45	4.89 E-4	0.45
55	1.48 E-4	0.40 (1)
65	3.08 E-4	0.43 (1)
80	4.59 E-4	0.45 (1)

Notes: (1): Did not stabilize at the end of test, value is only used for curve fitting Fickian curves to data.

Table 4.9 Fickian diffussion parameters for the Hardcore 12-inch FRP

Water temperature (^{o} C)	Diffusivity, D (cm^2/hr)	Saturation moisture, M_∞ (%)
22	8.17 E-6	0.19
35	1.99 E-5	0.19
45	1.52 E-5	0.27
55	4.81 E-5	0.22
65	6.08 E-5	0.18
80	1.17 E-5	0.50 (1)

Notes: (1): Did not stabilize at the end of test, value is only used for curve fitting Fickian curves to data.

Table 4.10 Fickian diffussion parameters for the Hardcore 24-inch FRP

Water temperature (^{o} C)	Diffusivity, D (cm^2/hr)	Saturation moisture, M_∞ (%)
22	1.16 E-4	0.21
35	7.85 E-5	0.26
45	4.42 E-5	0.26
55	9.54 E-5	0.24
65	2.30 E-4	0.26
80	1.70 E-4	0.26 (1)

Notes: (1): Did not stabilize at the end of test, value is only used for curve fitting Fickian curves to data.

4.3.4.3 Measured Properties as a function of submergence time and moisture

The effect of time of submergence and moisture on the mechanical properties of the FRP tubes was evaluated by performing longitudinal and hoop tension tests on specimens aged in 22^o C water for submergence times ranging between 4 and 787 days. Typically, five or more specimens were tested at each submergence period. The tests were carried out using the same procedure used to determine the baseline properties.

Variations of the mechanical properties of the aged FRP samples are presented in the following subsections. The results are presented normalized with respect to the baseline property values.

4.3.4.3.1 Aged properties for Lancaster 24-inch FRP tube

Variations of the longitudinal and hoop properties versus submergence time for this FRP shell are shown in Figures 4.17 and 4.18, respectively. The error bars shown in these figures correspond to ± one standard deviation. Longitudinal tensile test results on this particular FRP composite shell showed no evidence of significant degradation of property

values. This is likely related in part to the fiber orientation of this composite $(\pm 35^{o}/85^{o}/\pm 35^{o})_{T}$, which makes it a matrix dominated composite in the longitudinal direction, and also possibly due to a gain of ductility of the matrix upon immersion in water. Tensile properties in the hoop direction showed some degradation, but it was not very significant. The hoop tensile strength decrease by about 8 %. The error bars shown in these figures indicate considerable scatter.

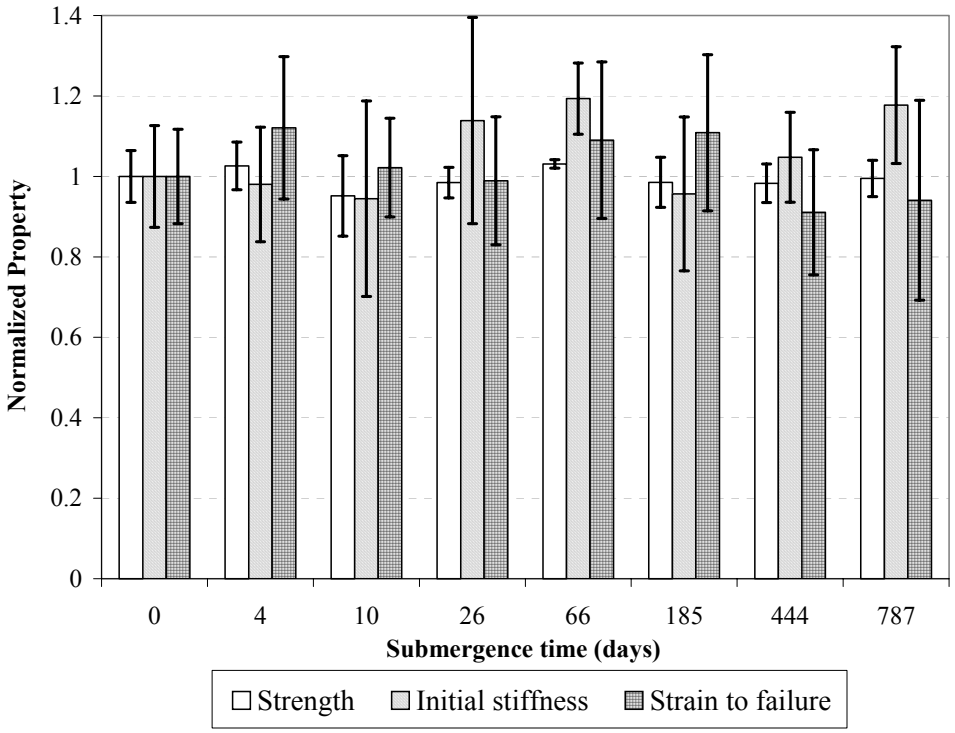

Figure 4.17 Longitudinal tensile properties versus submergence time for Lancaster 24-inch FRP tube

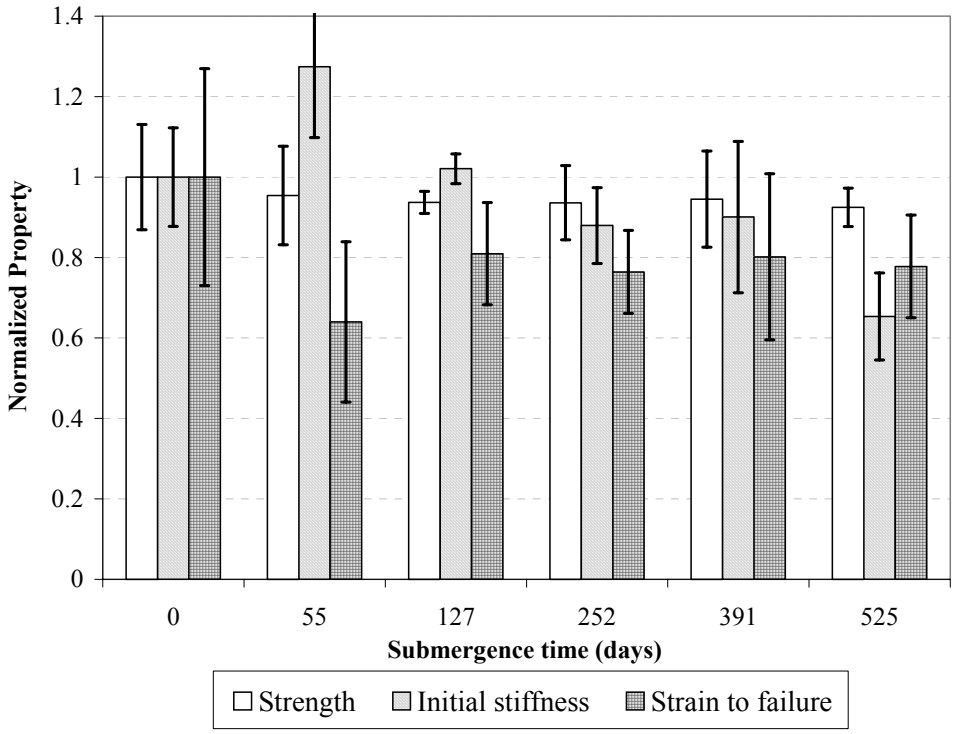

Figure 4.18 Hoop tensile properties versus submergence time for Lancaster 24-inch FRP tube

4.3.4.3.2 Aged properties for Lancaster 12-inch FRP tube

The longitudinal and hoop properties versus submergence time for this FRP shell are shown in Figures 4.19 and 4.20, respectively.

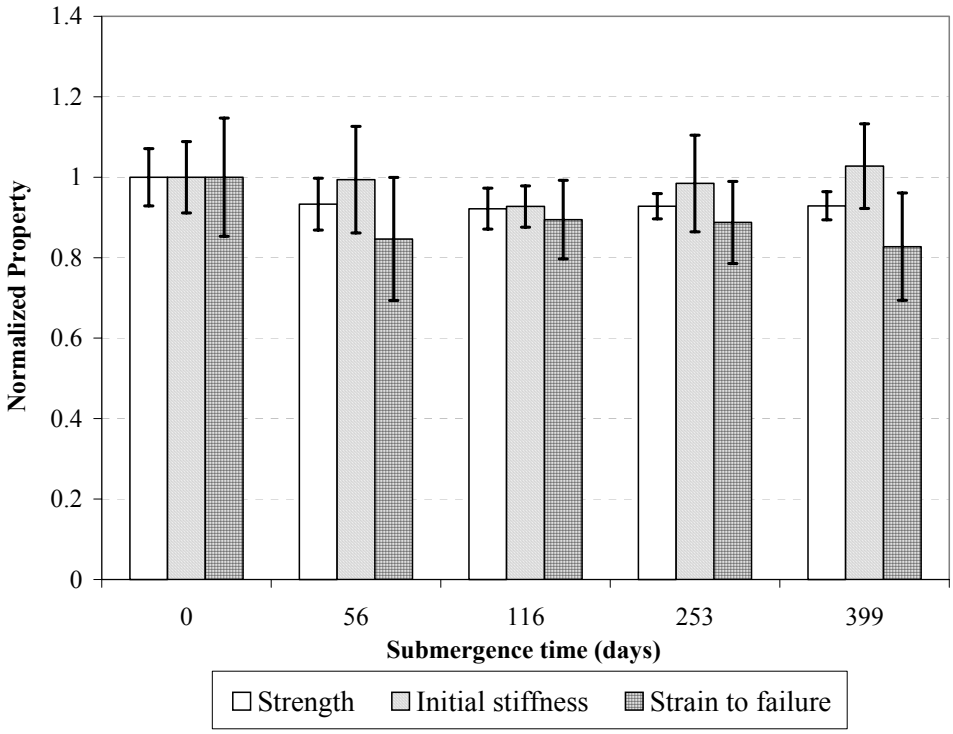

Figure 4.19 Longitudinal tensile properties versus submergence time for Lancaster 12-inch FRP

Figure 4.19 shows that after approximately 400 days of submergence in fresh water at 22^{o} C, the longitudinal tensile strength and strain to failure decreased about 9 and 18%, respectively. The initial stiffness (in the 0 to 4000 microstrain range) remained almost constant.

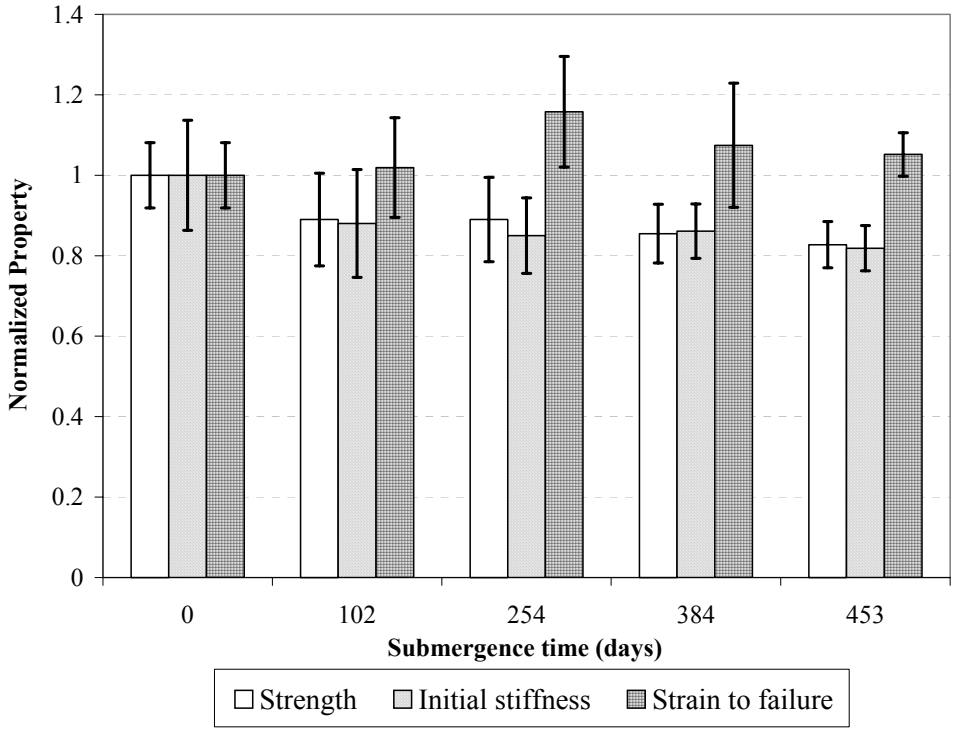

Figure 4.20 Hoop tensile properties versus submergence time for Lancaster 12-inch FRP

Figures 4.20 shows that the hoop tensile strength and initial stiffness decreased about 17% and 18%, respectively. Degradation levels for strength and stiffness are more significant for the 12-inch compared to the 24-inch, because the fiber lay-up of the 12-inch composite is more fiber dominated. However, the strain to failure did not change much.

Strength and stiffness versus percent moisture absorption are shown in Figures 4.21 and 4.22 for the longitudinal and hoop directions, respectively. Both figures show tensile strength decreases with increasing moisture content, but the strength values tend to stabilize at higher moisture contents. The hoop tensile stiffness showed a similar behavior, as shown in Figure 4.22b. These plots are useful for predicting mechanical properties versus time, as shown later in this chapter.

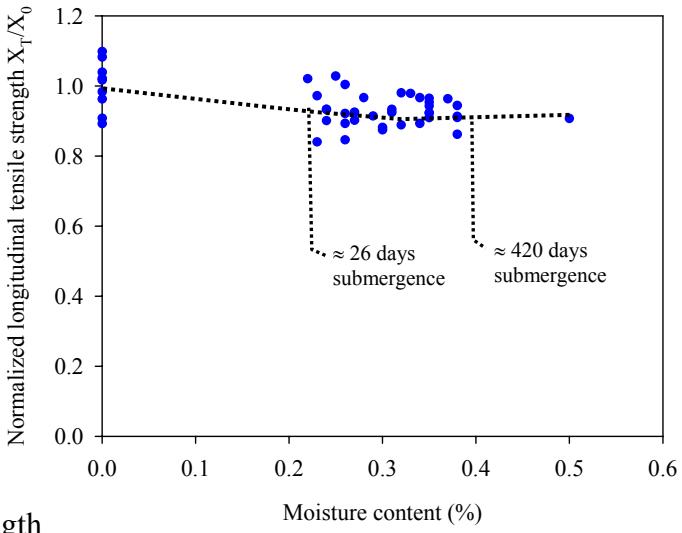

a) Variation of strength

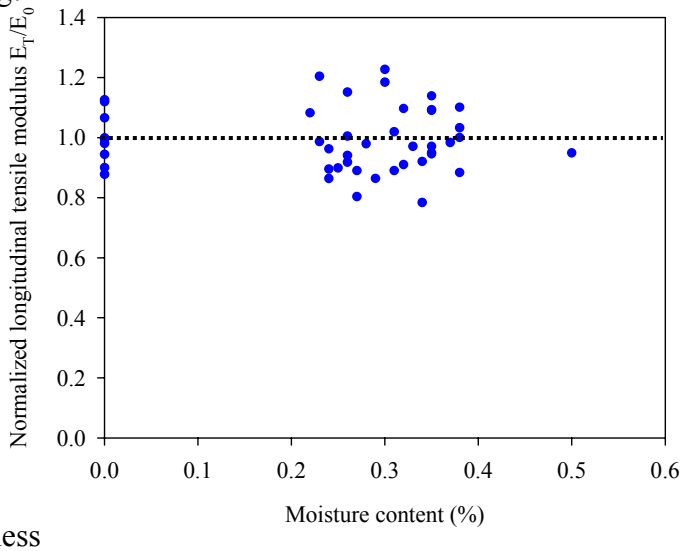

b) Variation of stiffness

Figure 4.21 Longitudinal tensile properties versus moisture content for Lancaster 12-inch FRP tube

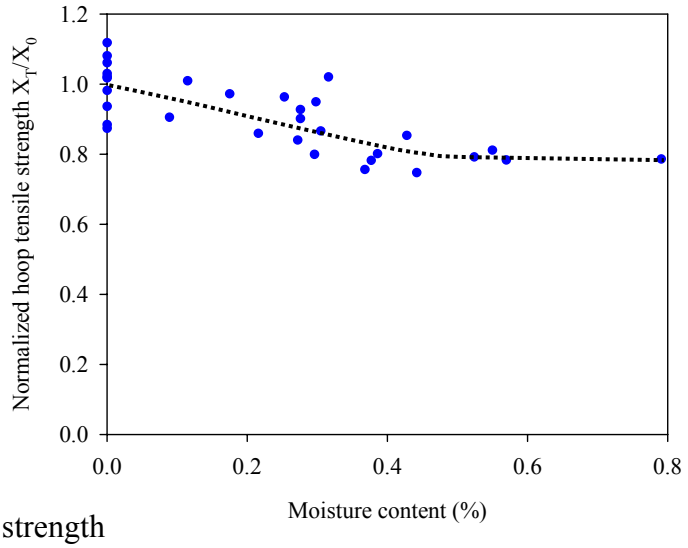

a) Variation of strength

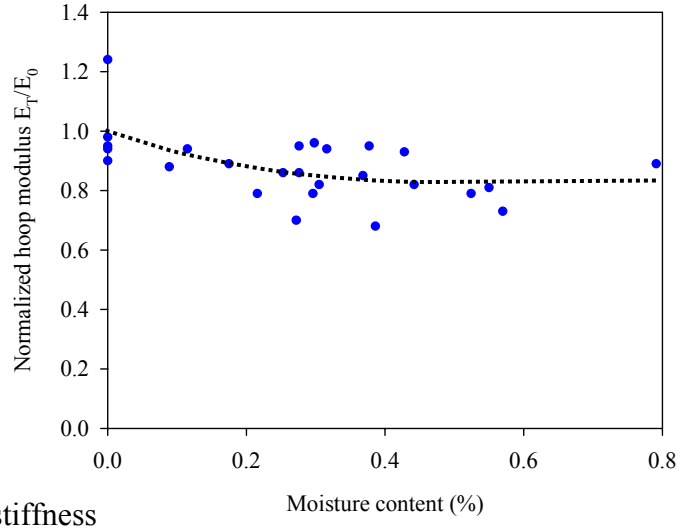

b) Variation of stiffness

Figure 4.22 Hoop tensile properties versus moisture content for Lancaster 12-inch FRP

4.3.4.3.3 Aged properties for Hardcore 24-inch FRP tube

The longitudinal properties versus submergence time for this FRP shell are shown in Figure 4.23.

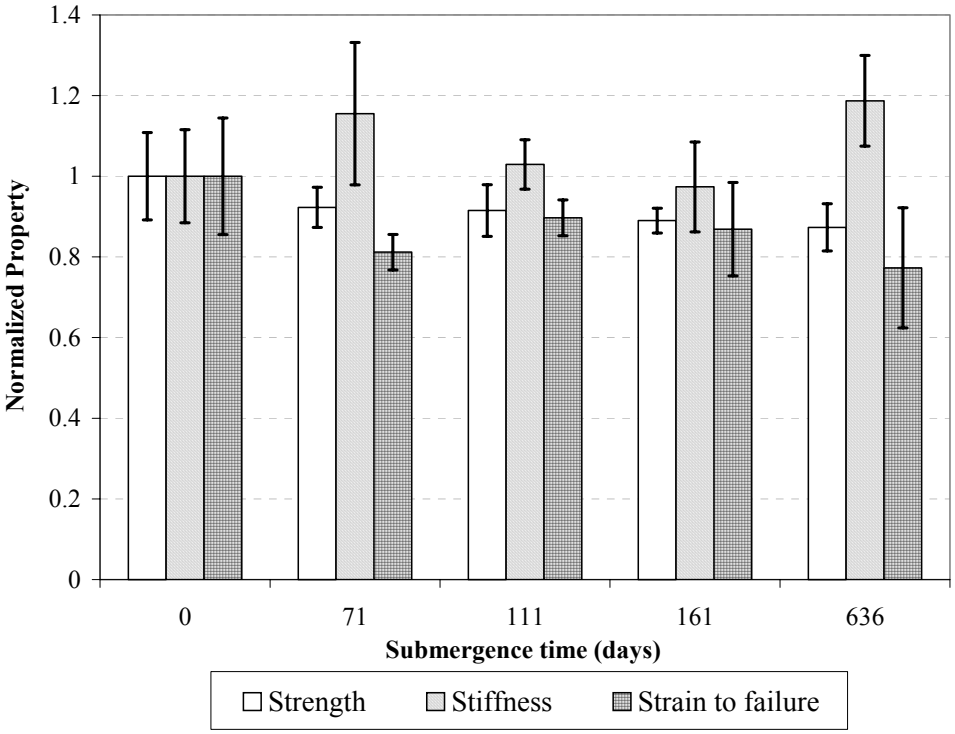

Figure 4.23 Longitudinal tensile properties versus submergence time for Hardcore 24-inch FRP

The above figure shows that after approximately 636 days of submergence in fresh water at 22^{o} C, the longitudinal tensile strength decreased about 13%. The strain to failure decreased by about 20 %. The initial stiffness values (0 to 4000 microstrains) did not show a clear trend with respect to the baseline values. The error bars shown indicate that the strain and stiffness values had considerable scatter.

The variation of the longitudinal tensile strength and stiffness versus percent moisture absorption are shown in Figures 4.24. This figure shows a tensile strength loss of about 16 % at the highest moisture content value of 0.33 %. The initial stiffness values show considerable scatter and no clear trend can be determined.

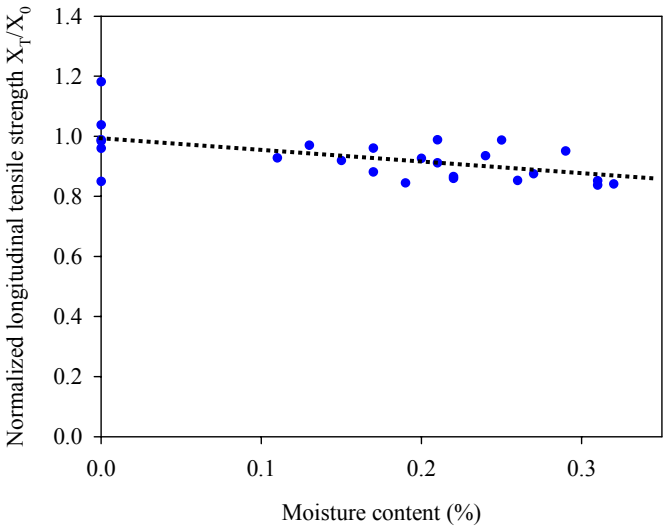

a) Variation of strength

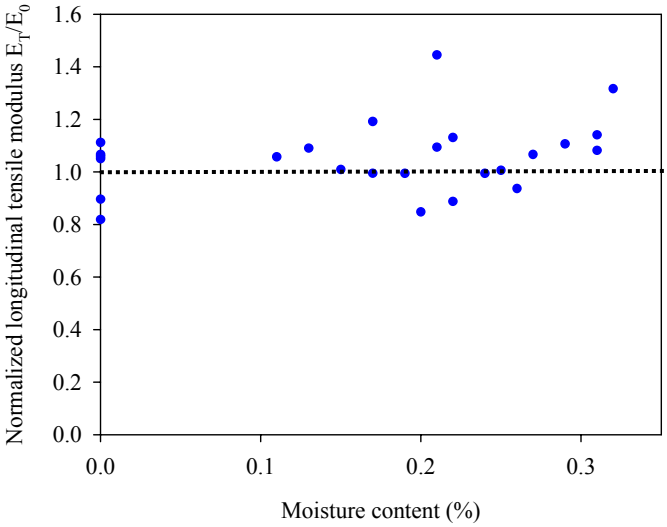

b) Variation of stiffness

Figure 4.24 Longitudinal tensile properties versus moisture content for Hardcore 24-inch FRP tube

4.3.4.3.4 Aged properties for Hardcore 12-inch FRP tube

The longitudinal and hoop tensile properties versus submergence time for this FRP shell are shown in Figures 4.25 and 4.26, respectively.

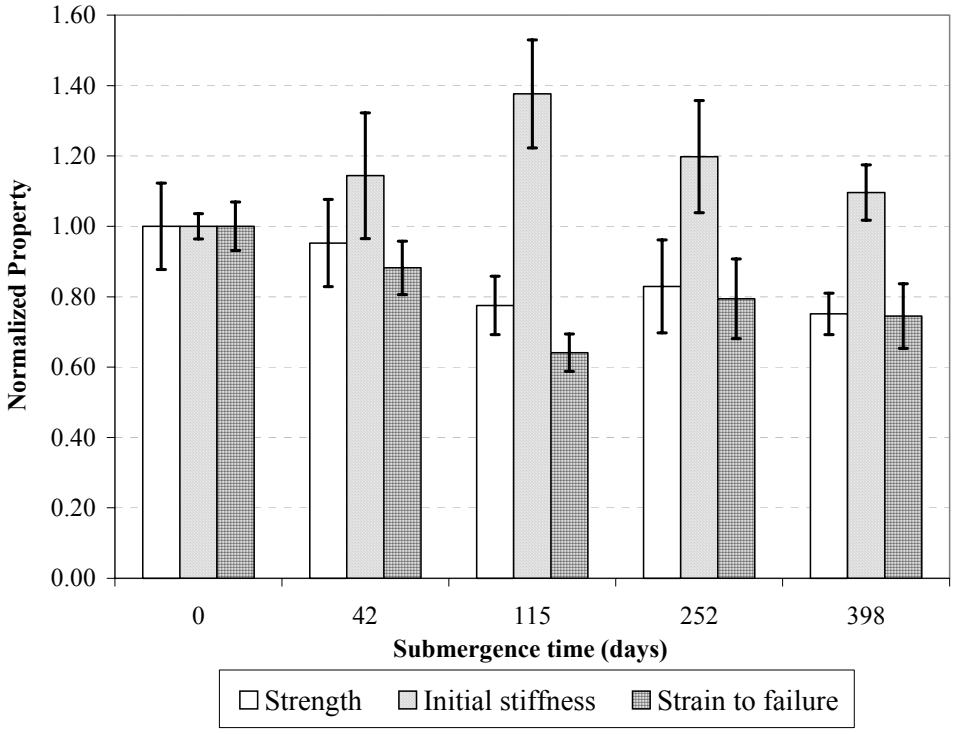

Figure 4.25 Longitudinal tensile properties versus submergence time for Hardcore 12-inch FRP

Figure 4.25 shows that after approximately 398 days of submergence in fresh water at 22^{o} C, the longitudinal tensile strength and strain to failure decreased by about 24 % and 25%, respectively. The initial stiffness increased by about 10%.

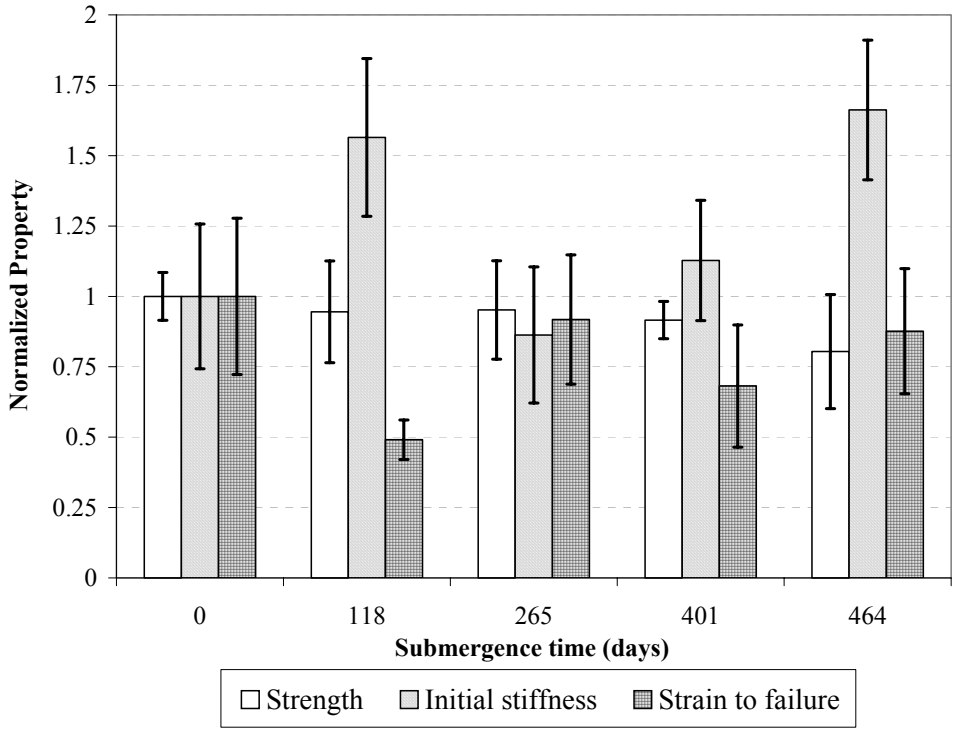

Figure 4.26 Hoop tensile properties versus submergence time for Hardcore 12-inch FRP

Figure 4.26 shows that after approximately 464 days of submergence in fresh water at 22^{o} C, the hoop tensile strength decreased by about 20%. The stiffness and strain to failure values showed very high scatter. This could be related to material variability. Another possible reason could be related to the infusion tubes used to inject the resin during manufacturing of the FRP tubes. These tubes were removed prior to hoop split disk testing, however at these locations the FRP shell wall thickness increased and decreased sharply within a small distance. It is possible that high stress concentrations occurred at these locations and affected the results.

The variation of tensile strength and stiffness versus percent of moisture absorption, for the longitudinal and hoop directions are shown in Figures 4.27 and 4.28, respectively.

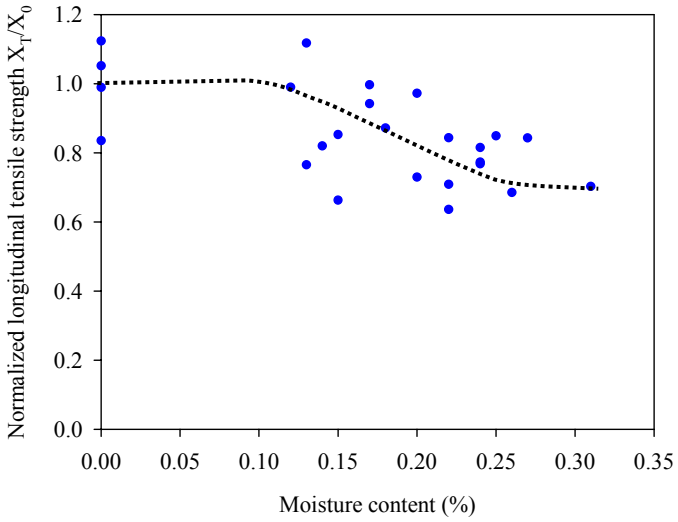

a) Variation of strength

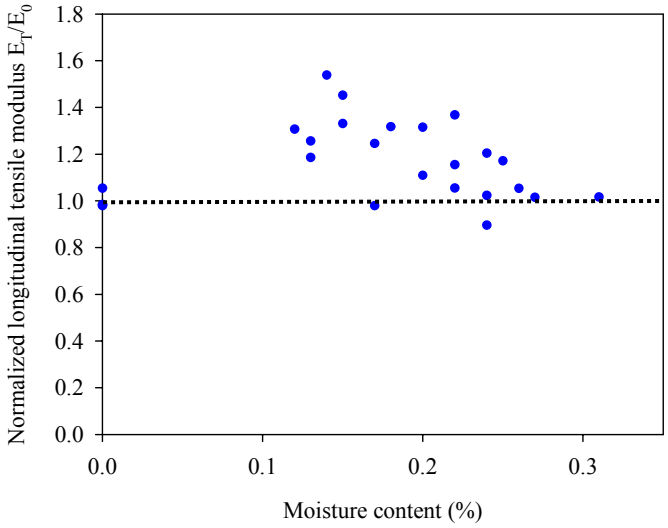

b) Variation of stiffness

Figure 4.27 Longitudinal tensile properties versus moisture content for Hardcore 12-inch FRP tube

As shown in Figure 4.27 a, the longitudinal tensile strength decreases with increasing moisture content. The maximum tensile strength degradation was about 25 % at a moisture content of about 0.25 %. No clear trend was observed between longitudinal tensile modulus and moisture content.

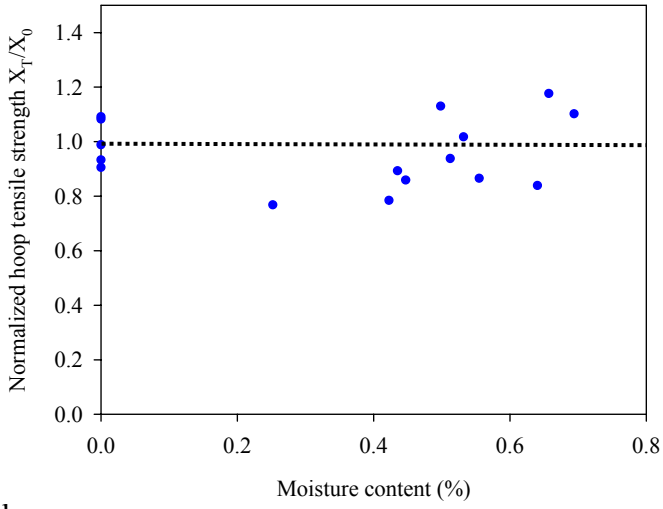

a) Variation of strength

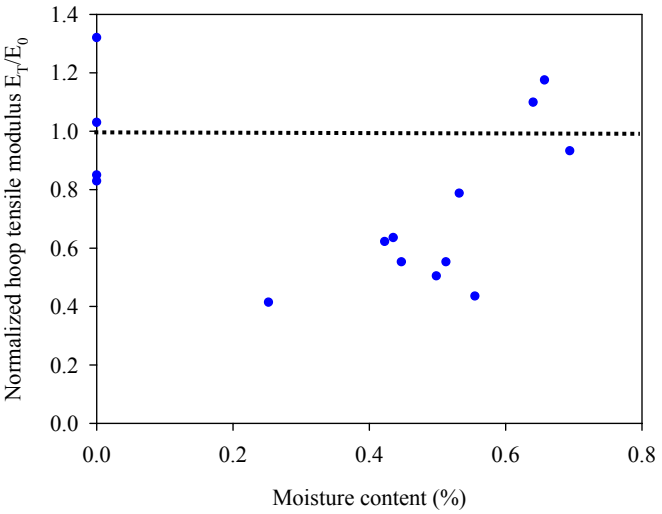

b) Variation of stiffness

Figure 4.28 Hoop tensile properties versus moisture content for Hardcore 12-inch FRP tube

Figure 4.28 shows very high scatter for hoop tensile strength and stiffness, hence no clear relationship was observed with moisture content. As mentioned before, the high scatter in the hoop tensile properties for the 12-inch Hardcore shell could be related to material variability, and the sharp variations of FRP shell wall thickness near the location of the resin infusion tubes which possibly created high stress concentrations and affected the results.

4.3.5 Freeze-thaw degradation of saturated FRP samples

Longitudinal tensile tests were performed on saturated coupon samples after 0, 100, 300, and 500 freeze-thaw cycles. The saturated coupons refer to specimens that were soaked in 22^{o} C water until they reached moisture content at saturation, i.e., M_{∞} (see Figures 4.9 through 4.12 for the time of soaking required to reach M_{∞}). Three or more samples were tested at each stage. The typical temperature cycle undergone by the specimens is shown in Figure 4.6. The specimens were cycled between -17^{o} C and + 6^{o} C, and the duration of each cycle was about 2.4 hours. The test setup is described in Section 4.3.2.4.

The results are presented in Figures 4.29 through 4.32. These figures are normalized with respect to the properties obtained from samples submerged in 22^{o} C water, at or near the saturation moisture content, M_{∞}.

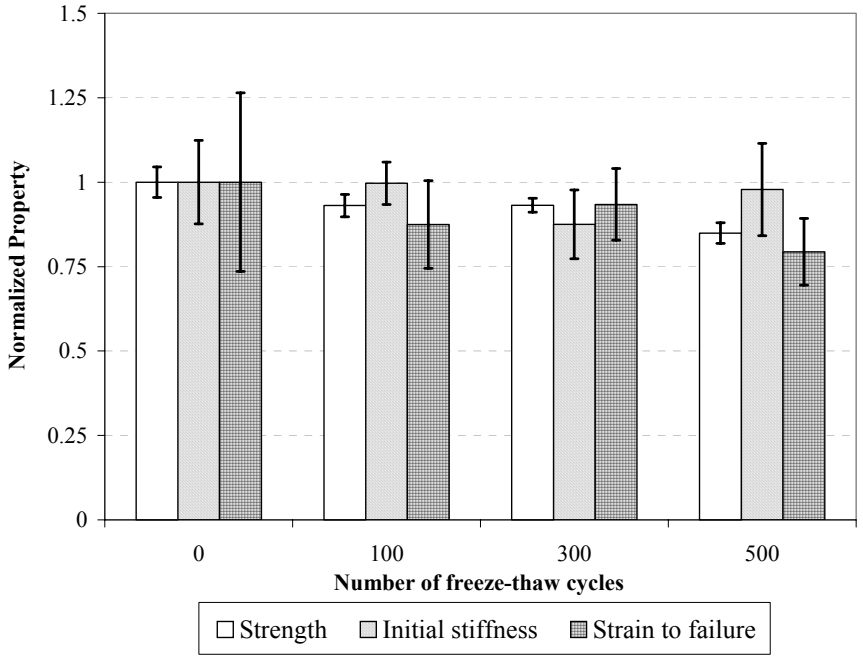

Figure 4.29 Influence of freeze-thaw cycling on the longitudinal tensile properties for the Lancaster 24-inch FRP

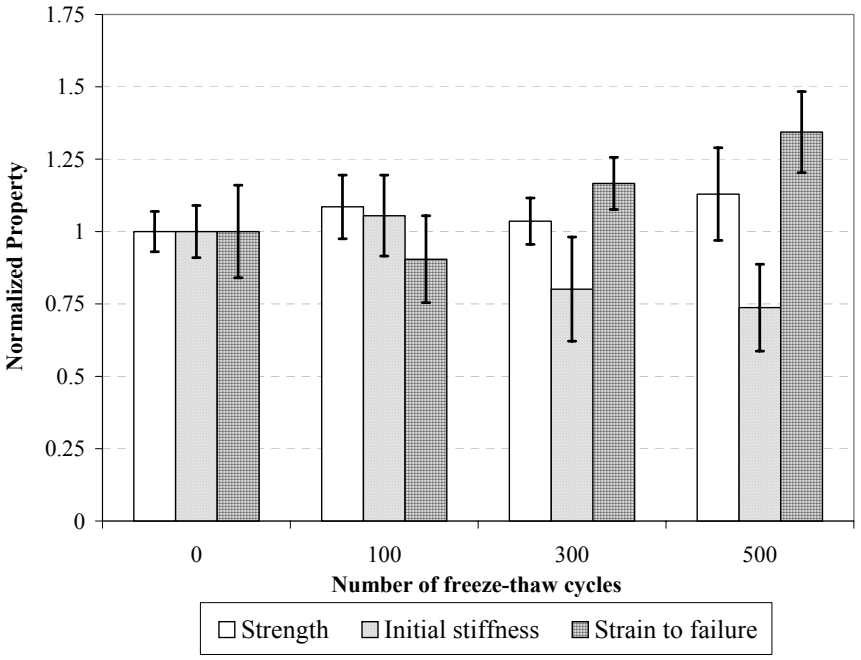

Figure 4.30 Influence of freeze-thaw cycling on the longitudinal tensile properties for the Lancaster 12-inch FRP

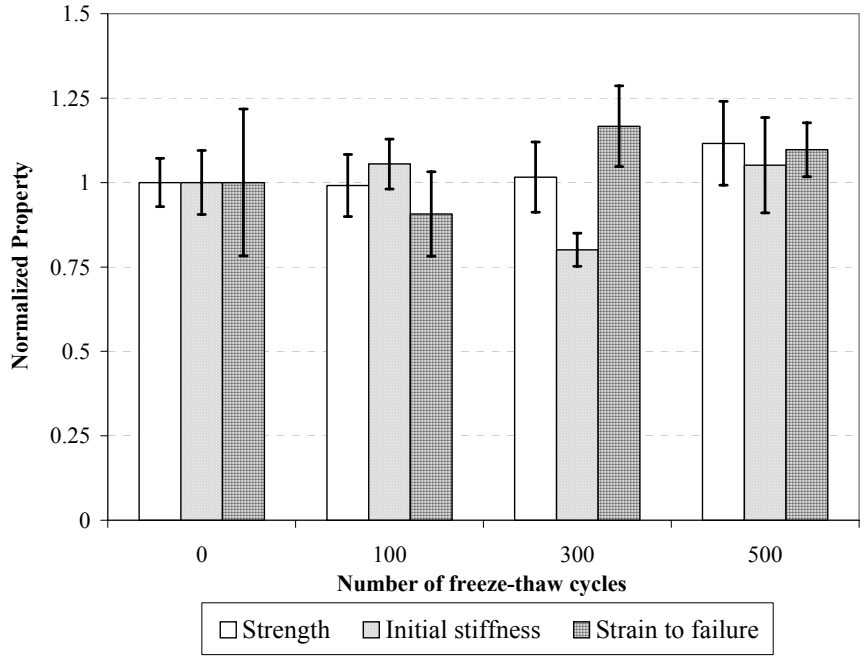

Figure 4.31 Influence of freeze-thaw cycling on the longitudinal tensile properties for the Hardcore 24-inch FRP

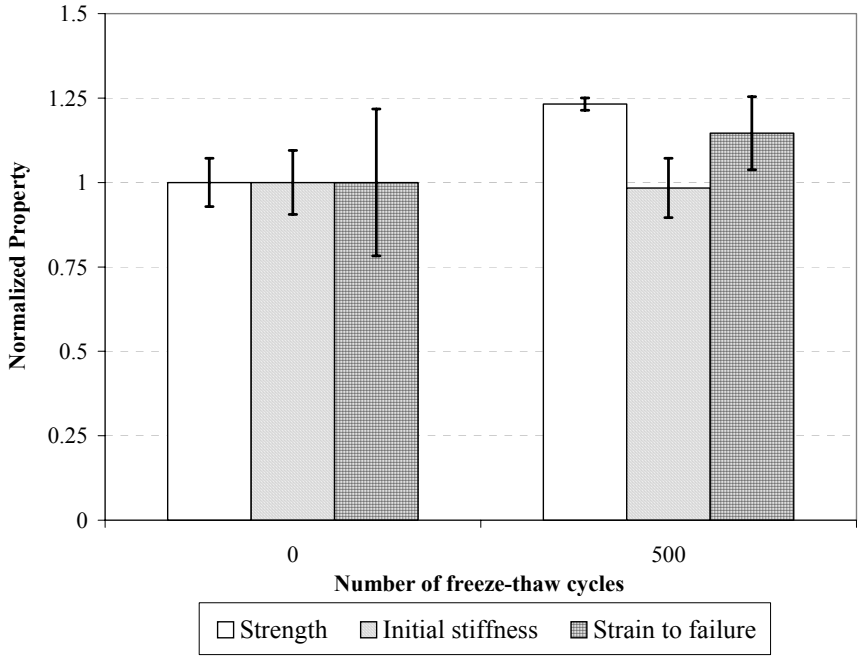

Figure 4.32 Influence of freeze-thaw cycling on the longitudinal tensile properties for the Hardcore 12-inch FRP

The freeze-thaw data indicates little change in the longitudinal tensile properties of the FRP tubes, except for Lancaster 24-inch where a strength decrease of about 20% was recorded after exposure to 500 freeze-thaw cycles.

4.3.6 SEM imaging

Scanning electron microscopy (SEM) was used to investigate the damage mechanisms for the FRP composite tubes. The SEM images allowed examination of the state of the fibers and the surrounding matrix at different exposure conditions used in the experimental program. For each FRP tube type, SEM micrographs were obtained for the following conditions: as-received, at the end of moisture absorption in 22^{o} C water (i.e. saturation), and after freeze-thaw cycling. SEM images for the four types of FRP tubes investigated are shown in Figures 4.33 through 4.36.

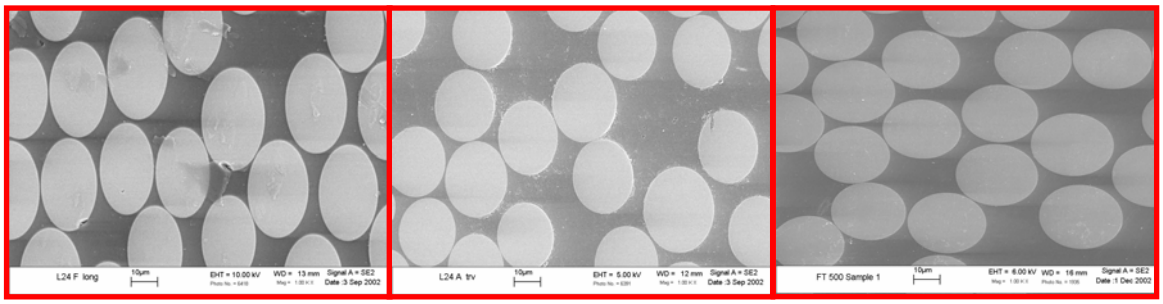

a) as-received condition b) at saturation moisture c) after 500 freeze-thaw cycles

(Note: magnification is x1000 for the three micrographs)

Figure 4.33 SEM images for Lancaster 24-inch FRP tube

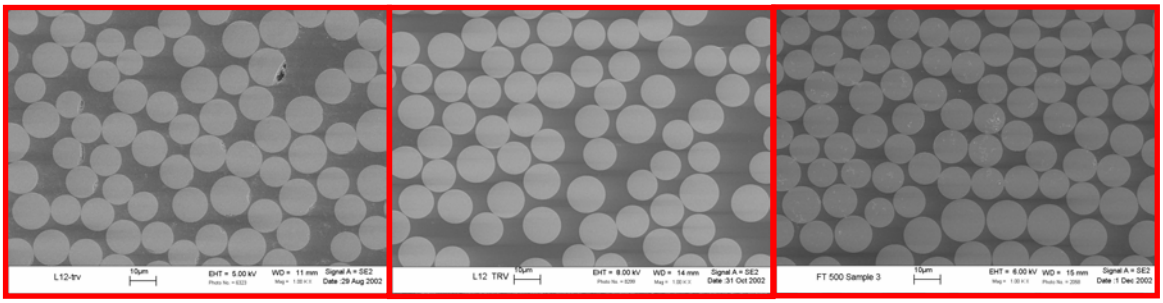

a) as-received condition b) at saturation moisture c) after 500 freeze-thaw cycles

(Note: magnification is x1000 for the three micrographs)

Figure 4.34 SEM images for Lancaster 12-inch FRP tube

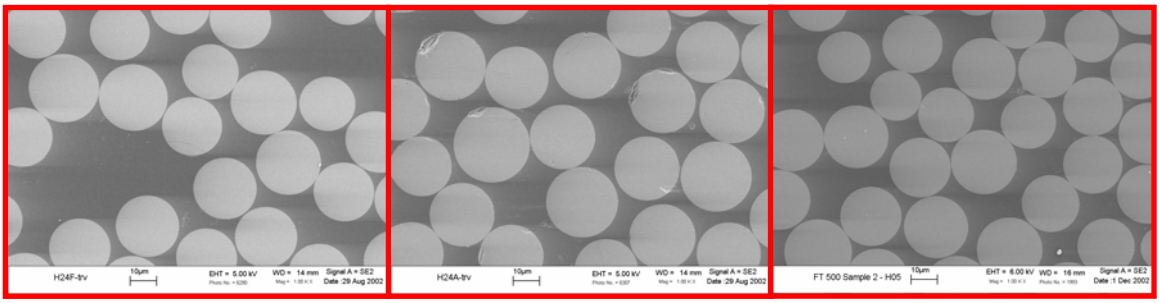

a) as-received condition b) at saturation moisture c) after 500 freeze-thaw cycles

(Note: magnification is x1000 for the three micrographs)

Figure 4.35 SEM images for Hardcore 24-inch FRP tube

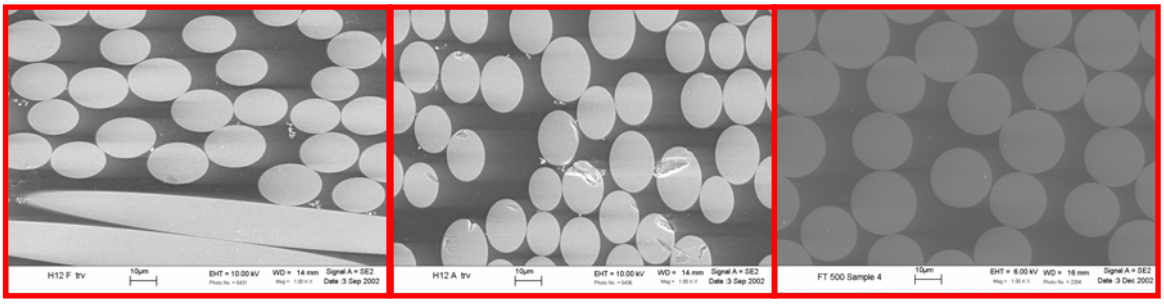

a) as-received condition b) at saturation moisture c) after 500 freeze-thaw cycles

(Note: magnification is x1000 for the three micrographs)

Figure 4.36 SEM images for Hardcore 12-inch FRP tube

Some damage was noticed in the SEM images taken at the saturation moisture state. The signs of degradation included damage at the fiber and at the interface between the fiber and matrix.

4.4 LONG TERM STRUCTURAL CAPACITY OF FRP COMPOSITE PILES

The durability experimental program described above was based on testing FRP coupons submerged in 22^{o} C water with their edges coated to approximate 1-D diffusion conditions. For a concrete-filled FRP pile, the diffusion will predominantly be in the radial direction. Furthermore, the boundary conditions on the inner and outer surfaces of the FRP shell of the pile will be different from the boundary conditions of the experimental program. A more realistic estimation of the FRP strength as a function of time can be modeled by calculating the average moisture content of the FRP shell using the approach described in Appendix B and in Pando et al. (2001). This approach involves calculating the moisture content of the FRP shell of the pile versus time using a radial moisture diffusion model and incorporating more appropriate boundary conditions. Once the relationship between the FRP shell moisture content and time is computed, one can calculate the FRP strength versus time relationships using the experimental data presented in Section 4.3. Although relationships of FRP properties versus time are useful, for estimating the long-term capacity we will only need the residual values for the FRP mechanical properties, i.e., the estimated long-term FRP properties.

4.4.1 Long term structural capacity of composite pile

This section presents a simplified example intended for illustrative purposes only, but it demonstrates the importance of considering evaluation of moisture aging effects on the FRP strength and stiffness (especially for bending capacity). A durability study involving tests on concrete-filled FRP stubs is currently underway (Lesko and Rizkalla 2003). The results from this study will help assess the validity of the durability model proposed here.

The long term structural capacity of concrete-filled FRP piles can be estimated using the short-term models for axial and flexural structural behavior by Fam and Rizkalla (2001, 2002), coupled with the long-term mechanical properties for the FRP tube after degradation has occurred. The long-term mechanical properties of the FRP tube can be estimated using experimental relationships between FRP properties and moisture content, such as the ones presented earlier in this chapter. The moisture content used to estimate the long-term FRP properties should correspond to the long-term average moisture concentration expected in the field for the FRP tube in the pile. A procedure to estimate the long-term moisture content for a cylindrical FRP is described in Appendix B and in Pando et al. (2002).

As an example, the long-term axial capacity for the 12-inch Lancaster pile is estimated. With the FRP dimensions and as-received properties presented in Section 4.3.3, and using the model by Fam and Rizkalla (2001), we obtain the axial load-strain response curve shown as a solid line in Figure 4.37. If we now assume a 25% and 40% long term reduction for the FRP hoop stiffness and strength, respectively, we obtain the long-term load-strain curve shown as the dashed line in this same figure (note these degradation values are higher than the measured degradation levels in this study). This represents approximately a 5 % ultimate (structural) axial capacity reduction.

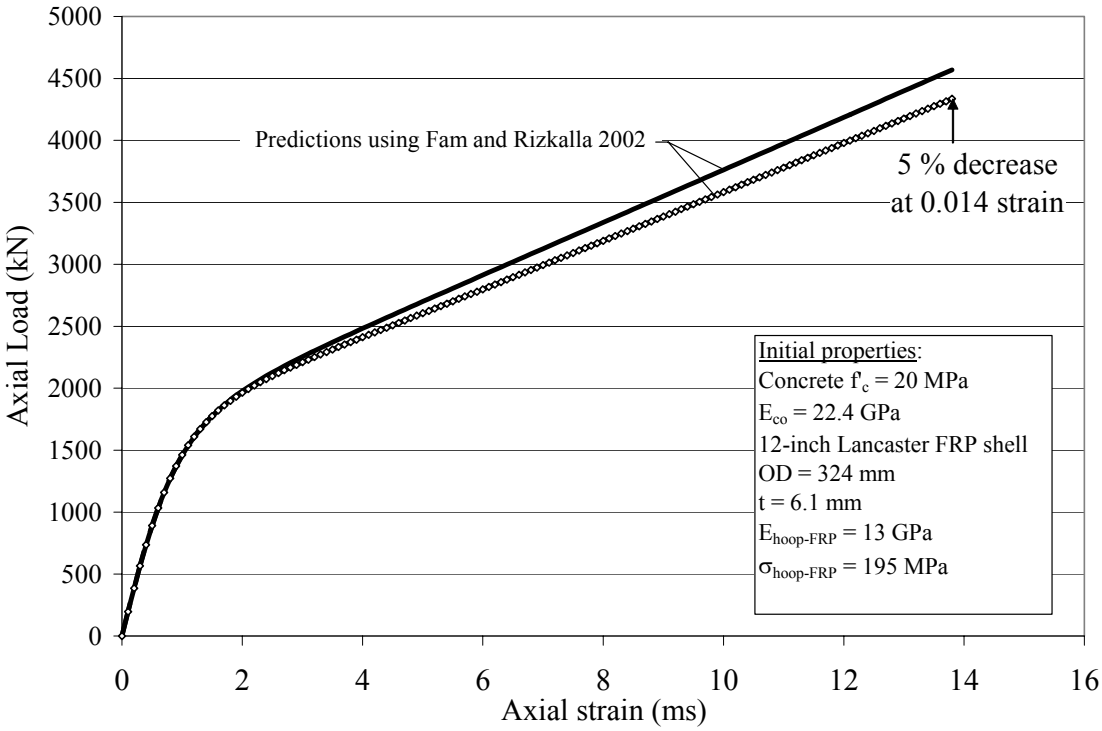

Figure 4.37 Estimated long-term axial capacity of the 12-inch Lancaster pile

As shown in Figure 4.37, the impact of degradation of the FRP mechanical properties on the long-term axial structural capacity of concrete-filled FRP composite piles is small due to the fact that the majority of the capacity contribution is from the concrete infill.

Similarly, the long-term flexural capacity (structural) for the same Lancaster pile can be predicted using Fam and Rizkalla (2002). The short-term moment-curvature response is shown as the solid line in Figure 4.38. Assuming similar stiffness and strength reduction levels as before, but in the longitudinal direction, we obtain the dashed moment-curvature line shown in Figure 4.38. This represents a 24 % reduction in the long term structural flexural capacity.

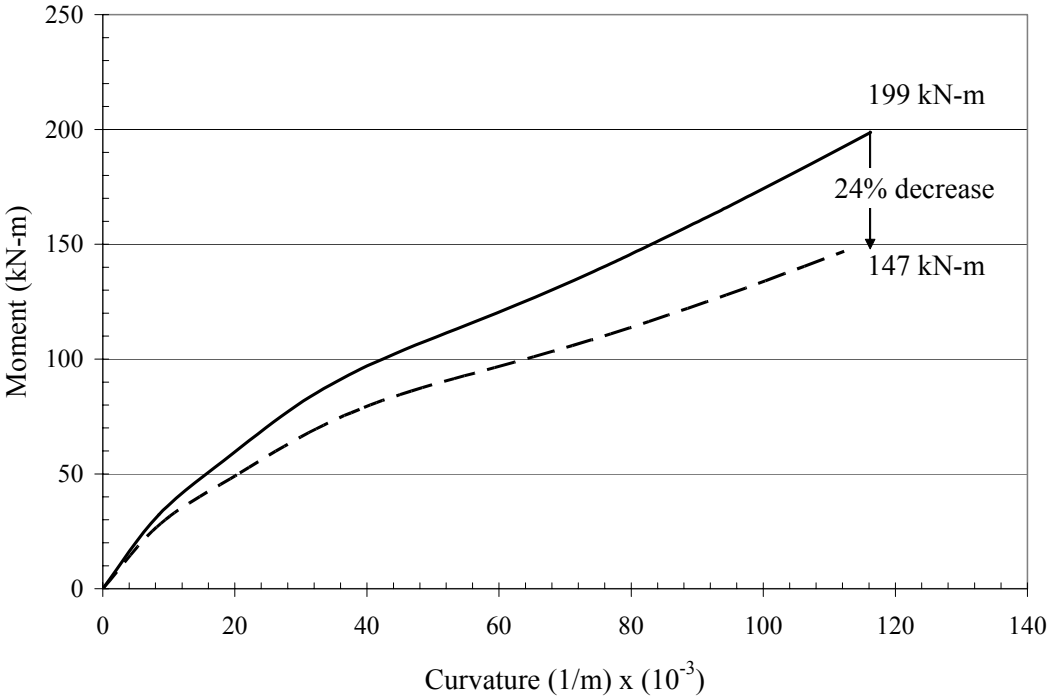

Figure 4.38 Estimated long-term flexural capacity of the 12-inch Lancaster pile

Figure 4.38, shows that the impact of FRP degradation is more significant for the flexural capacity because the FRP shell provides most of the capacity contribution on the tension side of the pile in flexion.

4.4.2 Comments related to the axial strain levels in piles

The structural ultimate limit state for axially loaded concrete-filled FRP columns or piles occurs at axial strain levels that exceed the normal range of ultimate strains typically used for normal unconfined concrete, e.g., 0.001 to 0.003. As shown in Chapter 2, and as reported by Fam and Rizkalla (2002) and others, the presence of the FRP shell allows this type of structural element to undergo much larger axial strains, e.g., to about 0.009 to 0.013. It is important to compare these strain levels to the strain levels that can be allowed to develop in a pile before serviceability limits are exceeded.

The strain distribution along the pile will depend on the soil conditions. A pile that develops all or most of its resistance from end bearing, such as piles with their tips founded on hard soil or rock, have almost a constant axial strain distribution with depth. For piles that develop their resistance from side friction, the strain will decrease with depth at a rate dependent on the side friction distribution along the pile length. The maximum strain in a pile will occur within the portion of the pile above the ground surface. The maximum axial strains in an axially loaded pile will be influenced by the allowable pile settlement determined from serviceability requirements. Typically the allowable settlement is between 25 and 50 mm (1 and 2 in.). For the case of an end-bearing pile with a allowable settlement of 37 mm, the length of the pile would have to be less than 12 m (40 ft) in order to develop axial strains in the pile above 0.003. For piles carrying their load purely in side friction, and with an allowable settlement of 37 mm, the length of the pile would have to be less than 24 m (81 ft) in order to start developing axial strains above 0.003. The pile lengths would have to be shorter if the allowable pile settlement is below 37 mm. This simple example illustrates how the additional strength and ductility provided by the FRP shell may not be utilized in the field for piles with serviceability requirements as above. Thus, serviceability may control design of FRP piles in many practical applications.

4.5 SUMMARY

A laboratory testing program was completed to study the long-term performance of FRP composite pipe piles. This durability study, which addressed the FRP shells of Lancaster and Hardcore composite piles, included FRP shell characterization, determination of baseline mechanical properties, measurement of moisture absorption as a function of time and temperature, measurement of mechanical properties as a function of moisture absorption, and measurement of mechanical properties as a function of freeze-thaw cycles.

From the results of the durability study, the following conclusions and observations were made:

- Moisture absorption has a small impact on the strength of some FRP composites, and a larger impact on others.

- Curve fits using the Fickian and Langmuirian models were perfomed on the experimental moisture absorption data gathered for the different FRP shells evaluated in this study. The results indicate that Langmuirian diffusion, which has four curve-fitting parameters (D, M_∞, α, β), is better able to track the measured moisture absorption than the Fickian diffusion, which has two-curve fitting parameters (D, M_∞), particularly for samples submerged at temperatures between 55 and 80^o C.

- The levels of strength degradation corresponding to steady state moisture contents reached after about 2.5 years of submergence were as follows:

    - Longitudinal tensile strength reductions on saturated FRP specimens were measured to be 0.5 , 7.1, 12.7, and 24.9 % for the Lancaster 24-inch, Lancaster 12-inch, Hardcore 24-inch, and Hardcore 12-inch, respectively.

    - Measured hoop tensile strength reductions due to moisture were 7.6, 17.3, and 19.6 % for the Lancaster 24-inch, Lancaster 12-inch, and Hardcore 12-inch, respectively.

- Degradation of longitudinal mechanical properties for the 24-inch Lancaster pile was not as significant as for the Hardcore pile because of the different fiber lay-ups. The Lancaster pile was matrix dominated in the longitudinal direction since the fibers with closest alignment to the longitudinal axis were 35 degrees off alignment.

- The impact of FRP degradation on the long term structural capacity of the piles was investigated using models by Fam and Rizkalla (2001 and 2002). This approach showed that, for a 12-inch diameter FRP pile, the axial structural capacity will decrease about 5% if the FRP tube hoop properties degrade 25% and 40% in stiffness and strength, respectively. The small impact that the FRP degradation has on the axial pile capacity is due to the fact that majority of the capacity contribution is coming from the concrete infill. The impact on larger diameter piles is expected to be even smaller. For the flexural capacity of a 12-inch pile, the results show that a 24% reduction in flexural capacity can be expected if the FRP tube longitudinal tensile properties degrade 25% and 40% in stiffness and strength, respectively. This result is as expected, because the concrete is weak in tension and the FRP tube provides the tensile reinforcement to the pile during bending.

- Exposure to freeze-thaw cycles was found to have little effect on the longitudinal tensile properties of the saturated FRP tubes. This is based on longitudinal tensile tests on samples exposed to 100, 300, and 500 freeze-thaw cycles.